Dilution Issues Related to Use of High Velocity Diffusers in Ocean Desalination Plants: Remedial Approach Applied to the West Basin Municipal Water District Master Plan for Sea Water Desalination Plants in Santa Monica Bay

Submitted by:
Scott A. Jenkins Consulting
14765 Kalapana St
Poway CA 92064

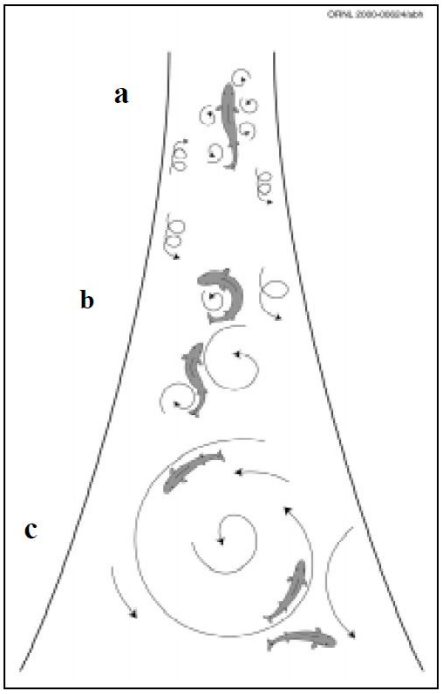

Submitted to:
Diane McKinney
Desalination Project Engineer
West Basin Municipal Water District
17140 S. Avalon Blvd., Suite 210
Carson, CA 90746

Revised: 30 May 2013

TABLE OF CONTENTS

EXECUTIVE SUMMARY

Published evidence is reviewed herein indicating that physical damage (due to turbulence and velocity shear pulling apart eggs, larva and small juveniles) occurs in open, free-stream turbulent environments, similar to what would occur when these organisms are entrained into the *turbulent mixing zone* of high velocity diffuser systems. We refer to this as *Turbulence Mortality*, and it occurs by two mechanisms. In the turbulent mixing zone of a diffuser, entrained eggs, larvae and juvenile adults suffer *impact mortality* from direct contact with the high velocity core of a diffuser jet. Along the outer edges of the high velocity core of a diffuser jet, *turbulent shear mortality* occurs along the streamlines between the entrainment and outflow regions of the turbulent mixing zone, where shearing rates in the fluid are very high. Remediation approaches previously applied to hydro-electric turbines, diversion channels and fish ladders by Cada and Glenn (2001) and Cada et al (2006) suggest that impact mortality can be minimized by lowering the velocities in the high speed core of a diffuser jet to a threshold impact velocity of about 1 m/ses; while turbulent shear mortality can be minimized by reducing shearing rates to less than $\frac{d\bar{u}}{dr} \leq 100 \text{ sec}^{-1}$, and by adjusting the Komogorov turbulent mixing lengths in the diffuser jet to significantly less than the size of the predominant organisms. We apply these previously tested remedial criteria to a redesign of the 20 mgd Phase-1diffuser from the Master Plan in order to minimize diffuser induced turbulence mortality.

Our approach to minimizing turbulence mortality is based on a species assessment and size distribution specific to mature larvae and juvenile adults life phases that was measured by Tenera Environmental at the intakes to the Redondo Beach Generating Station (RBGS) and the SeaLife intakes to the West Basin

Desalination Demonstration Facility; and from the intakes to the El Segundo Generating Station (ESGS) and Scattergood Generating Station. The size spectra of small organisms in the water column at these sites are very broad. It is not possible to both minimize jet velocity and shearing rate, while simultaneously making the Komogorov turbulent mixing lengths small relative to ***all*** resident water column species and life phases. Therefore it was necessary to prioritize the species size distribution in the Tenera data and focus on mature larvae and juvenile adult life phases. This size class of organism was chosen for this diffuser design optimization because it accounts for the life phases which have highest survival rates.

Seventeen separate design iterations were conducted with *COSMOS/ FLowWorks* to produce a modified 20 mgd Phase-1 diffuser design that minimizes turbulence mortality to mature larvae and juvenile adults. We refer to this modified design concept as the *Four-jet Rosetta Swirl-Chamber Diffuser* , and it was designed to plug into each of the five 10 inch diffuser riser pipes of the 20 mgd ARCADIS design in The Master Plan. In the modified design, the 10 inch riser pipes discharge at the seafloor interface into a 9 ft diameter swirl chamber that stands 3.8 ft above the sea floor and is fitted with four rigid 9.5 inch diameter low-velocity converging nozzle located in quadrature on the top of swirl chamber. The 3.8 ft high-stand of the swirl chamber above the seafloor isolates the discharge nozzles from large sand level variations or burial effects. Four pairs of "skid plates" atop the swirl chamber protect the converging nozzles from damage due bottom debris moving about in the wave surge or from boats dragging anchors. However, this configuration still allows divers to reach into the gap between the skid plates to service or replace the nozzles when needed.

Because the Four-jet Rosetta Swirl-Chamber Diffuser reduces the maximum discharge velocities by a factor of 4 relative to the original ARCADIS design in The Master Plan, the concern becomes whether or not it will produce adequate turbulence in the turbulent mixing zone in order to satisfy the water quality objects of either the present version of the *California Ocean Plan*, or the *5% Rule* under a potential amendment to The Ocean Plan. The purpose of the swirl chamber is to pre-empt turbulence formation in the brine effluent prior to discharge, rather than relying entirely on velocity shear between the discharge jet and the receiving water to generate turbulence, as occurs in the conventional ARCADIS design. The swirl chamber creates high in-the-pipe turbulence levels prior to discharge by two mechanisms. The first mechanism results from the very rapid flow divergence which occurs when the brine is discharged from the10 inch riser pipe into the 9 ft. diameter swirl chamber. This produces a rapid deceleration of the brine effluent against a large adverse pressure gradient inside the swirl chamber, a combination which produces flow instability and turbulence formation (Schlichting and Gersten, 1999). The second turbulence generating mechanism at work inside the swirl chamber is produced by a helical internal ribbing on the inner walls of the swirl chamber. This ribbing works like a screw, and causes the mass of brine fluid inside the chamber to rotate as it flows from the bottom of the chamber to the top, where the four discharge nozzles are located. The combined action of the flow divergence and flow rotation that occurs inside of the swirl chamber produces a turbulent brine effluent and provokes *turbulent cascading* to smaller mixing lengths prior to discharge (Schlichting and Gersten, 1999).

The pre-mature formation of high turbulence levels in the brine effluent inside the swirl chamber consumes flow energy, energy that must be provided by higher operating pressures in the discharge pipeline. “Quiet-ocean” CFD pipe flow

simulations indicate that the pressure requirements to drive the discharge hydraulic infrastructure against ambient ocean pressure increase from 6 psi over ambient for the 20 mgd ARACADIS design in The Master Plan to 8 psi over ambient when each of the five risers is fitted with the Four-jet Rosetta Swirl-Chamber Diffuser concept.

The quadrature arrangement of the jets on each Rosetta Swirl-Chamber Diffuser produces a turbulent mixing zone having considerable breadth , and consequently ocupies more aggregate volume of the receiving water than would otherwise be possible with a 20 mgd linear array of five single jet diffusers, as originally specified for the Phase-1 project in The Master Plan. With the Rosetta Swirl-Chamber Diffusers, the maximum velocities anywhere in the agregate turbulent mixing zone is $u_{\max}$ = 0.95 m /s; while the maximum shear rates anywhere in the turbulent mixing zone is $\frac{d\bar{u}}{dr}$ = 59 $\sec^{-1}$. Thus the combined discharges from five the Four-jet Rosetta Swirl-Chamber Diffusers at 30 ft. spacings will satisfy the threshold impact velocity criteria ($u_{\max} \leq 1$ m/sec) for eliminating impact mortality, while minimizing turbulent shear mortality by reducing shearing rates to less than $\frac{d\bar{u}}{dr} \leq$ 100 $\sec^{-1}$ Moreover, Komogorov turbulent length scales in the agregate turbulent mixing zone of five Rosetta Swirl-Chamber Diffusers are 20 times smaller than the smallest organism (1.5 mm) found in the Tenera species size distribution. Additionally, 99% of the turbulent energy in the agregate turbulent mixing zone occurs at turbulent length scales smaller than the smallest organism (1.5 mm). Therefore, all requirements for minimizing impact mortality and turbulent shear mortality have been satisfied by the Four-jet Rosetta Swirl-Chamber Diffuser concept, according to the minimization criteria set forth in Cada and Glenn (2001) and Cada et al (2006) that

was based on research conducted in the hydroelectic industry for fresh water species.

None of the brine plumes from the Four-jet Rosetta Swirl-Chamber Diffusers will broach the sea surface at either of the Redondo or El Segundo sites. This represents another improvement over the original ARCADIS high velocity diffuser design, whose brine plumes broached the surface at the shallow Redondo Beach site. Dilution performance of the Four-jet Rosetta Swirl-Chamber Diffuser is not as good as the original ARCADIS high velocity diffuser design in the Master Plan. The Four-jet Rosetta Swirl-Chamber Diffuser concept will none the less easily satisfy the discharge requirements of the present version of the California Ocean Plan, as well as the proposed 5 % rule amendment. Exposure times of drifting organisms to the brine plumes at very high salinity levels (45 ppt to 55 ppt) are about 5 minutes longer with the *Four-jet Rosetta Swirl-Chamber Diffuser*, as compared to the ARCADIS Phase-1 diffuser, although the exposure times for both designs are less than 1 hour at 45 ppt and less than 10 minutes at 55 ppt.

The Four-jet Rosetta Swirl-Chamber Diffuser was derived from turbulence mortality minimization criteria developed for fresh water species. The decisive question remains whether or not those citeria are valid for relevant local marine species. We recommend that the State Water Resources Control Board examine this question further.

ACKNOLEDGEMENT:

The *Four-jet Rosetta Swirl-Chamber Diffuser* concept is a derivative of an original design by GHD Engineering of Australia. The new features developed and presented herein by the authors are modified dimensions and the helical internal ribbing on the inner walls of the *swirl chamber* designed to provoke turbulent cascading of mixing lengths prior to discharge.

1.0) Introduction to Discharge Issues:

Hyper-salinity toxicity: The hydrodynamic aspects of this issue are the dilution and dispersion of the brine effluent discharged from the desalination plant diffusers. There are two regulatory discharge compliance questions related to brine dilution: 1) Will the diffuser discharges satisfy the 0.3 TUa objective of Requirement III.C.4(b) of the present version of the *California Ocean Plan* as it would apply to a *Zone of Initial Dilution* (ZID); and, 2) Will the diffuser discharges satisfy suggested amendments to the California Ocean Plan based on a recently released study by the California Water Resources Control Board Science Advisory Panel. Suggested amendments to the California Ocean Plan based on this report could set a numeric water quality objective limited to 5% over ambient ocean salinity at the limit of a *Regulatory Mixing Zone* measuring 100 m (330 ft) in radius around the discharge (referred to as the 5% rule). The Master Plan study Jenkins and Wasyl (2012) found that the 20 mgd Phase 1 discharge riser/diffuser design by ARCADIS easily satisfies both the present 0.3 TUa discharge water quality objective of Requirement III.C.4(b) of the California Ocean Plan, as well as the potentially more restrictive 5% rule (under a proposed future amendment to the California Ocean Plan) with its 100 m Regulatory Mixing Zone. The issue addressed in the present study is whether some modification to this design can be found that minimizes *turbulence mortality* associated with conventional high velocity diffuser systems.

Turbulence mortality: Physical damage (due to turbulence and velocity shear) may occur when planktonic organisms are entrained into the turbulent mixing zone of high velocity diffuser systems. Discharge jet velocities from the brine diffusers are on the order of 3 m/sec to 5 m/sec, generally higher than naturally occurring ocean currents. In the turbulent mixing zone of a diffuser, entrained eggs and larvae may suffer *impact mortality* from direct contact with the

high velocity core of a diffuser jet; and *turbulent shear mortality* in the entrainment and outflow regions of the turbulent mixing zone.

Bottom turbidity: The turbulent mixing zone of high velocity diffuser systems may cause re-suspension of bottom sediments and the formation of a bottom turbidity layer. This turbidity layer has the potential to cause impairment of the recruitment and growth of kelp beds on neighboring hard bottom substrate. Suspended sediment anomalies in the bottom turbidity layers were evaluated in The Master Plan studies (Jenkins and Wasyl, 2012) for the worst case 60 mgd Phase-2 diffuser discharge. No significant impacts to ambient light levels at the edges of the *Regulatory Mixing Zone* were found as a result of worst-case diffuser induced bottom turbidity.

2.0) Diffuser Turbulence Mortality:

In the Brine Panel Report, (Jenkins, et. al. 2012), diffuser-based discharge strategies are presented as *a preferred discharge technology*. An alternative to this technology is the use of in-plant dilution for desalination facilities that are co-located with once-through sea water circulation systems. Nothing in EPA regulations, EPA guidance, or the California Ocean Plan prohibits the use of in-plant dilution or blending for purposes of reducing salinity concentrations at the point of discharge. However, the primary concern with this alternative disposal strategy is mortality to micro-organisms (eggs and larvae) arising from the velocity shear and turbulence effects of the pump impellors in once-through sea water circulation systems, (Bamber and Seaby, 2004). This is generally referred to as *Entrainment Mortality*, but should probably be further distinguished as *Confined Entrainment Mortality*. This qualifier should be applied because there exists published evidence that this same sort of physical damage (due to turbulence and velocity shear pulling apart eggs and larva) can also occur in open, free-stream

turbulent environments, similar to what would occur when these organisms are entrained into the *turbulent mixing zone* of high velocity diffuser systems. Herein we will refer to this as *Free-jet Entrainment Mortality*, indicating such mortality can also occur in the unconfined spaces of the interior water column of the receiving water body.

The effect of turbulence on larval mortality was studied in the field by Jessopp (2007), who found that even turbulent *tidal flows* produce significantly increased mortality to thin-shelled veligers of gastropods and bivalves. The 20 mgd Phase-1 discharge jets produce axial discharge velocities of 3.4 m/sec; while as much as 4.3 m/sec occur in the core of 60 mgd Phase-2 diffuser jets (cf: Figure 1.1,

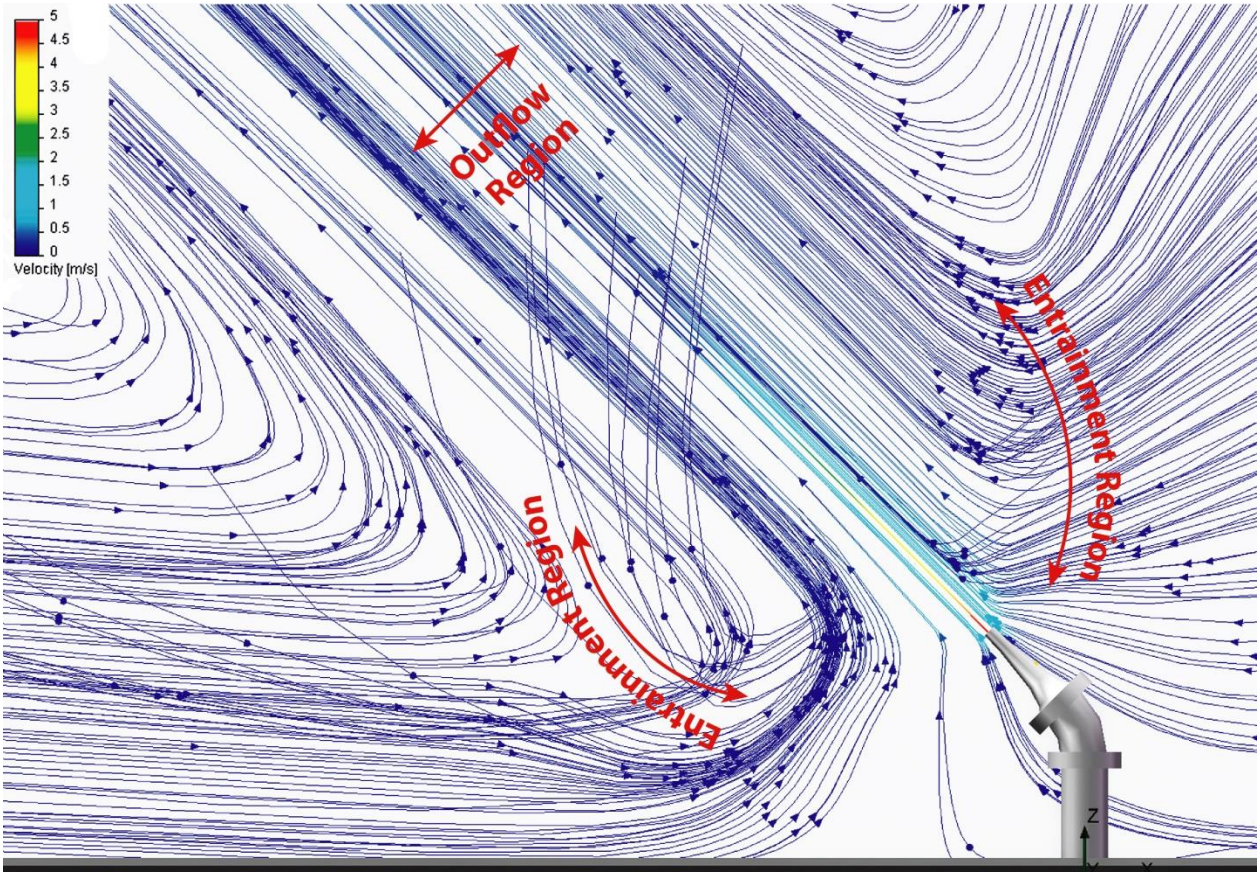

Figure 1.1: Hydrodynamic simulation of outflow and entrainment regions in the nearfield of a Phase-2 diffuser riser. Total Phase-2 discharge: 5 nozzles x 12 mgd ea. = 60 mgd total brine discharge at 67 ppt end-of-pipe.

Jenkins and Wasyl, 2012). Velocities of this magnitude are significantly greater than naturally occurring ocean currents; and exceed the threshold for *impact mortality* of most ichthyoplankton. However, the turbulence from these high velocity jets effect relatively small areas of receiving water on the order of tens of square meters (the turbulent mixing zone). Regardless, the area of a typical turbulent mixing zone is significantly greater than the cross section of an intake pipe to a once-through sea water circulation system.

In the turbulent mixing zone of a diffuser, entrained eggs, larvae and juvenile adults suffer *impact mortality* from direct contact with the high velocity core of a diffuser jet, (where the high velocity core of the discharge jet of a 60 mgd Phase-2 discharge jet produces axial discharge velocities of 4.3 m/sec; cf. Figure 1.1). Figure 1.2 shows that the high velocity core is relatively narrow in lateral extend, generally on the order 3 to 5 discharge port diameters. Along the outer edges of the high velocity core of a diffuser jet, *turbulent shear mortality* occurs along the streamlines between the entrainment and outflow regions of the turbulent mixing zone, where shearing rates in the fluid are very high. Here the mean rate of

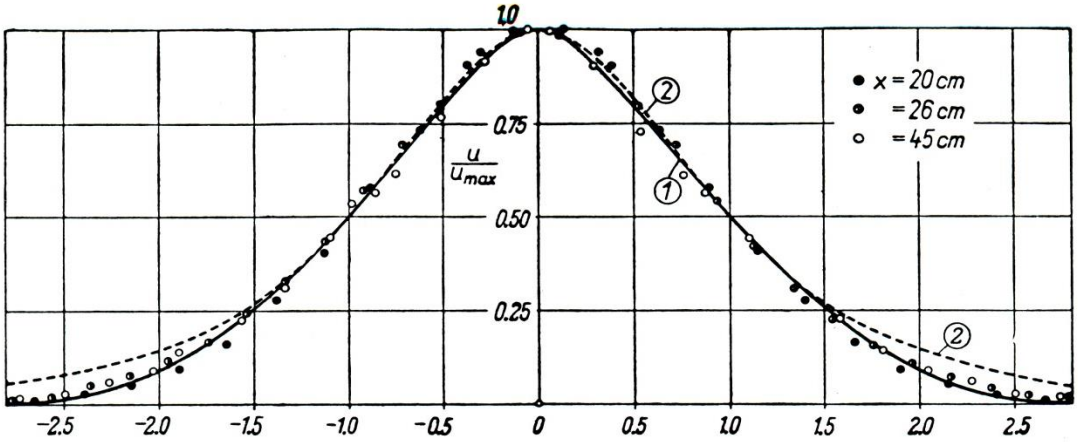

Figure 1.2: Non-dimensional velocity distribution across the high speed core of a circular, turbulent jet (Schlichting and Gersten 1999).

shear for the Phase-1 diffuser jets is $\frac{d\bar{u}}{dr} \cong \ 1.3514\, u_{\max} / d_{\min} = 200$ sec $^{-1}$; and $\frac{d\bar{u}}{dr} \cong$ 340 sec $^{-1}$ for the Phase-2 diffuser jets, cf. Figure 1.2. (Here $u_{\max}$ is the maximum discharge velocity, and $d_{\min}$ is the minimum port gap opening of the Tideflex nozzles.) these high shearing rates marine eggs, larvae, soft shelled veligers, and juvenile adults are particularly vulnerable to becoming distorted, sheared or ripped apart, particularly when the size of the affected organisms are comparable to the Komogorov turbulent mixing lengths.

The Komogorov turbulent mixing lengths are the length scales of those particular turbulent velocity fluctuations at which the preponderance of turbulent kinetic energy is dissipated. Figure 1.3 gives a visualization of Komogorov turbulent mixing lengths by means of shadow-graphic techniques applied to a densely stratified turbulent jet, similar to a brine plume. Figure 1.4b shows schematically the hyper-distortion and shearing that occurs to organisms whose sizes are comparable to Komogorov turbulent mixing lengths. Because most of the turbulent flow energy is concentrated on the organism's body at these mixing lengths, turbulent shear mortality results. If the organism is large in comparison to the Komogorov turbulent mixing lengths (as shown schematically in Figure 1.4a) then turbulent mixing causes a *scrubbing* action that varies along the length of the organism's body, but does not result in full-body distortion as is the case in Figure 1.4b. Therefore turbulent shear mortality generally does not occur if the organism is large in relation to Komogorov turbulent mixing lengths. On the other hand, if the organism is small in relation to Komogorov turbulent mixing lengths (Figure 1.4c) then the organism can be twirled, rotated and disoriented by turbulent mixing action with a higher probability of mortality occurring from behavioral dis-

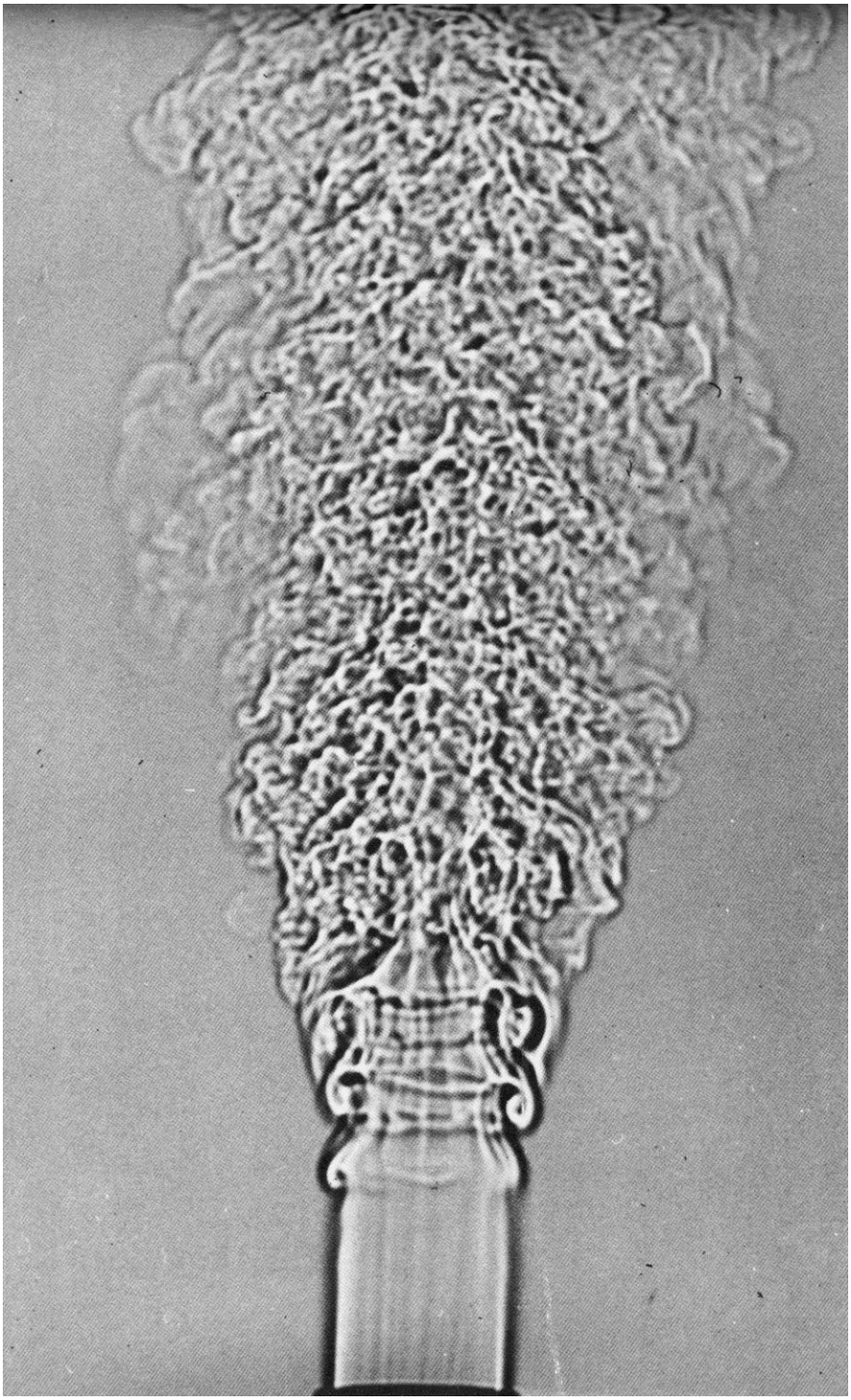

Figure 1.3: Shadowgraph of turbulent velocity fluctuations (eddies) in a dense (stratified) turbulent jet, revealing size of Komogorov turbulent mixing lengths; (from Schlichting and Gersten, 1999).

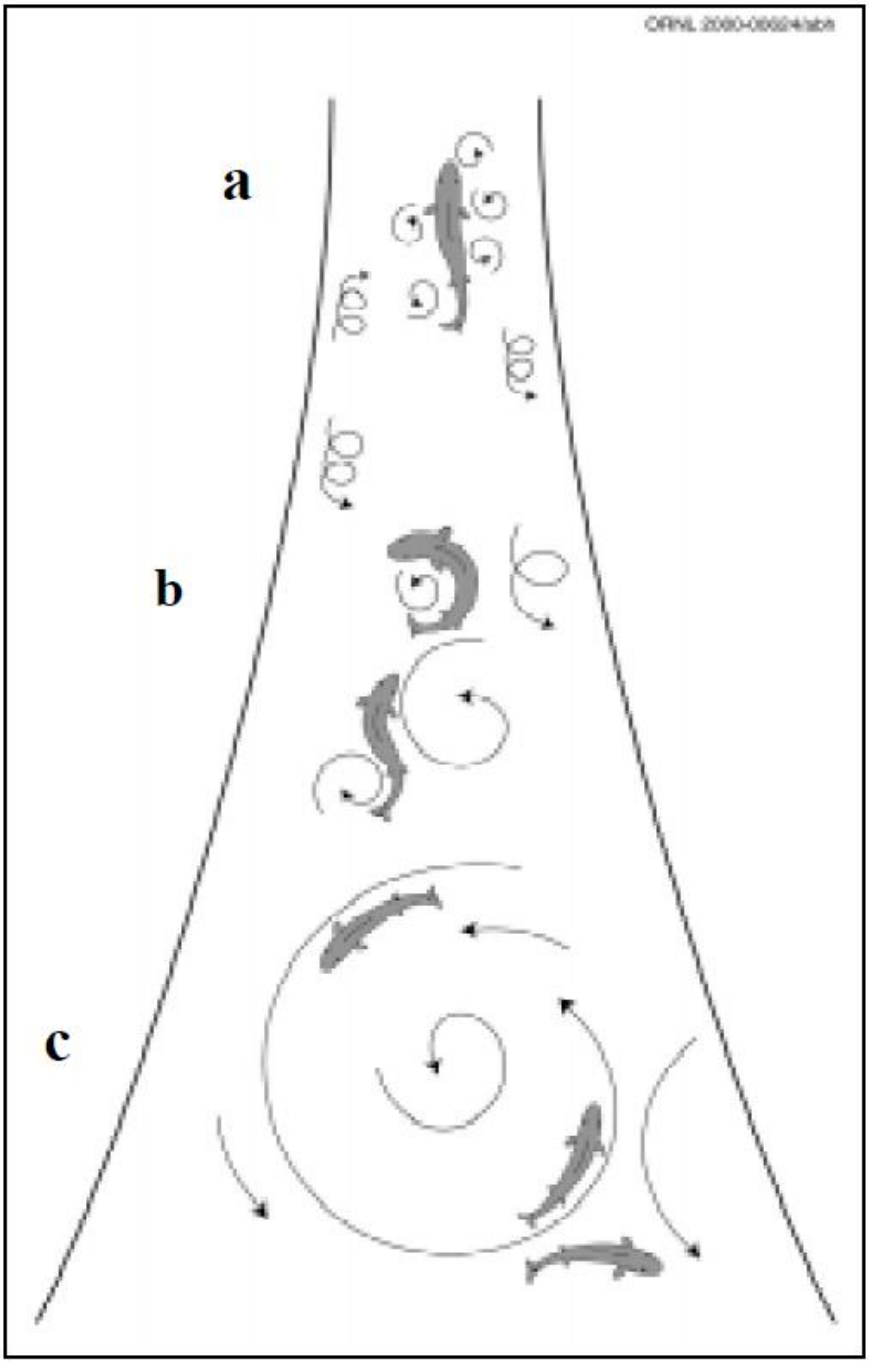

Figure 1.4: Relationship between size of marine organism and turbulent mixing length scales: a) Organism large relative to Komogorov turbulent mixing length; b) Organism comparable to Komogorov turbulent mixing length; and c) Organism small relative to Komogorov turbulent mixing length, from Cada, (2001)

function. Therefore the ideal set of discharge turbulence length scales that minimizes turbulence mortality results from a diffuser that generates low shearing rates and Komogorov turbulent mixing lengths that are small in relation to the resident organisms in the water column.

Remediation approaches previously applied to hydro-electric turbines, diversion channels and fish ladders by Cada and Glenn (2001) and Cada et al (2006) suggest that impact mortality can be minimized by lowering the velocities in the high speed core of a diffuser jet to a threshold impact velocity of about 1 m/ses; while turbulent shear mortality can be minimized by reducing shearing rates to less than $\frac{d\bar{u}}{dr} \leq 100 \text{ sec}^{-1}$, and by adjusting the Komogorov turbulent mixing lengths in the diffuser jet to significantly less size of the predominant organisms, as shown schematically in Figure 1.2a. We will adopt this approach in the present study, focusing our attention on redesigning the 20-mgd diffuser design to achieve diffuser core jet velocities, shearing rates and turbulent mixing lengths within these parameter limits, as adopted from hydro-electric turbulent flow applications.

3.0) Species Type and Size Assessment Specific to Master Plan Sites:

Our approach to minimizing turbulence mortality is based on a species assessment and size distribution specific to mature larvae and juvenile adults life phases that was measured by Tenera Environmental at the intakes to the Redondo Beach Generating Station (RBGS) and the SeaLife intakes to the West Basin Desalination Demonstration Facility (APPENDIX-A), and from the intakes to the El Segundo Generating Station (ESGS) and Scattergood Generating Station (APPENDIX-B) . The RBGS and ESGS are the two sites evaluated in The Master Plan (2012). The

size spectra of small organisms in the water column at these sites is very broad. It is not possible to both minimize jet velocity and shearing rate, while simultaneously making the Komogorov turbulent mixing lengths small relative to ***all*** resident water column species and life phases. Therefore it was necessary to prioritize the species size distribution in the Tenera data and focus on mature larvae and juvenile adult life phases, as listed in APPENDIX A & B. This size class of organism was chosen for this diffuser design optimization because it accounts for the life phases which have highest survival rates. This portioning of the turbulence mortality minimization exercise is required to obtain closure in the diffuser turbulence equations.

Figure 2.1 gives the probability density (red) and cumulative probability (black) of mature larvae and juvenile adults life phases. These probability distributions are based on 67 species at the intakes to the Redondo Beach Generating Station (RBGS) and the SeaLife intakes to the West Basin Desalination Demonstration Facility from APPENDIX-A; and on 73 species from the intakes to the El Segundo Generating Station (ESGS) and Scattergood Generating Station in APPENDIX-B. The median length of this ensemble of organisms is 2.5 mm, while the smallest size class is 1.5 mm. The largest organism is in the 10.5 mm size class, but these rare, with a probability of occurrence of about 0.1%. Therefore, in order to minimize the turbulent shear mortality of the mature larvae and juvenile adults life phases, we need to modify the Phase-1 20 mgd diffuser design to generate Komogorov turbulent mixing lengths substantially smaller than 1.5 mm, and ideally about an order of magnitude less.

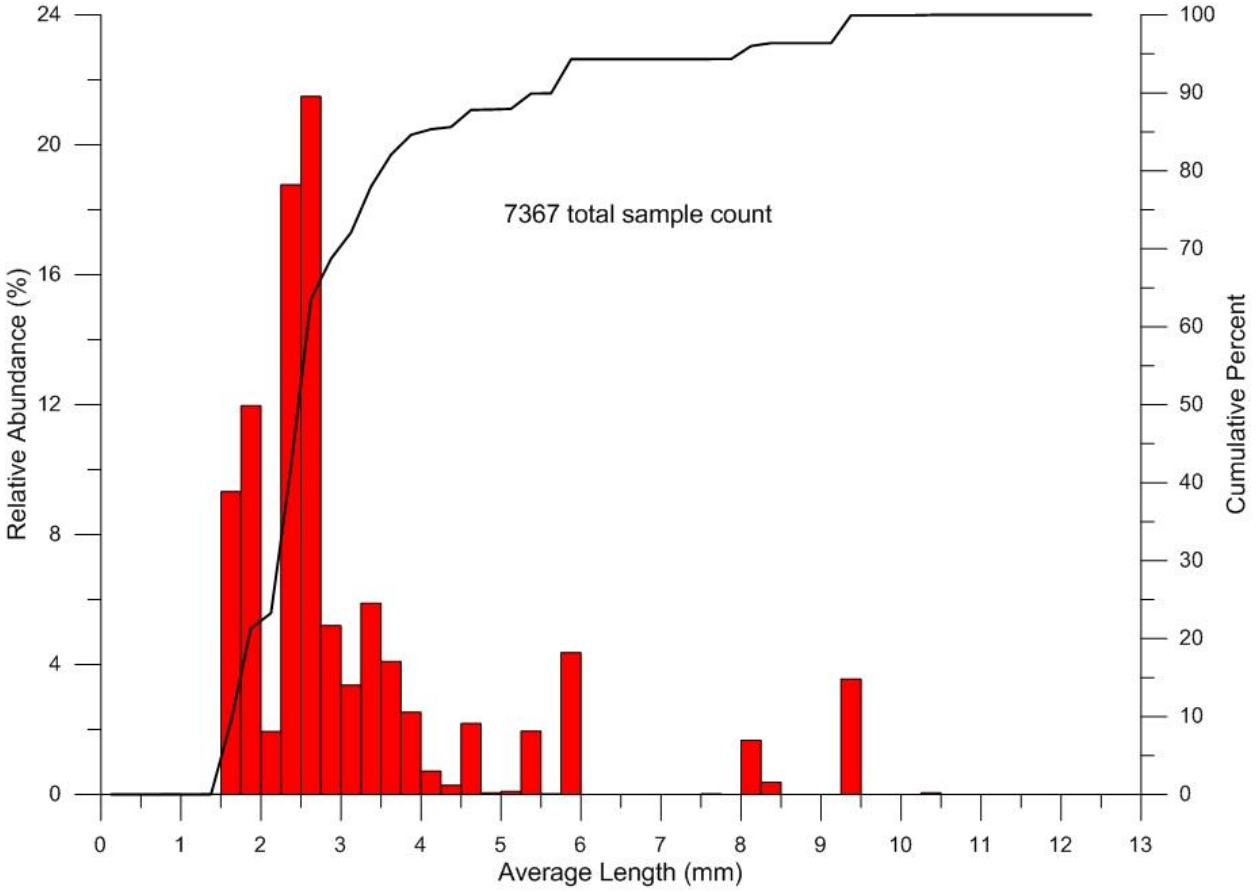

Figure 3.1: Probability density (red) and cumulative probability (black) of mature larvae and juvenile adults life phases. Based on 67 species at the intakes to the Redondo Beach Generating Station (RBGS) and the SeaLife intakes to the West Basin Desalination Demonstration Facility (APPENDIX-A); and on 73 species from the intakes to the El Segundo Generating Station (ESGS) and Scattergood Generating Station (APPENDIX-B).

4.0) Minimization of Turbulence Mortality of Phase-1 Diffusers:

The 20 mgd phase diffuser was redesigned to minimize turbulence mortality using four distinct hydrodynamic models. 1) The basic riser and diffuser internal flow simulations were performed using a commercially available hydraulics design software known as ***COSMOS/ FLowWorks***. Many design iterations were performed with this software until the desired combination of axial discharge velocity, shear rate and turbulence length scales were achieved at exit ports of the diffuser. 2) The subsequent kinetics of the discharge plume upon exiting the diffuser ports was evaluated using a computational fluid dynamics model, the ***Vortex Lattice CFD Model .*** This model computed the jet core velocities, shear rates and Komogorov turbulent mixing lengths in the outflow regions of the turbulent mixing zone as well as the flow structure of the entrainment region, see Figure 1.1 for definition of these brine plume flow regions. 3) The nearfield dilution performance of the new Phase -1 diffuser design was evaluated by another commercially available software known as ***Visual Plumes***, that has been certified by the U.S. Environmental Protection Agency and the California State Water Resources Control Board for use in diffuser design and nearfield dilution. 4) Finally, a fully 3-dimensional far field dispersion model ***SEDXPORT*** was used to assess the large scale trajectory of the brine plume. This model is a processed-based stratified flow model with the complete set of littoral transport physics including tidal transport, and wind & wave induced transport and mixing.

These models were powered by the same overlapping long-term records for the eight controlling model input variables used in The MasterPlan (2012) studies of Jenkins and Wasyl, (2012). These input variable time series were developed by

a process of *data fusion*. Data fusion involves merging archival data bases with site monitoring data of the marine environment in Santa Monica Bay.

4.1) Design Modification to the 20 mgd Phase-1 Diffuser: Seventeen separate design iterations were conducted with *COSMOS/ FLowWorks* to produce the modified 20 mgd diffuser concept shown in Figure 4.1 that achieves the design goals specified in Section 2 to minimize the turbulence mortality of the mature larvae and juvenile adults life phases detailed in Section 3. The four-jet Rosetta configuration in Figure 4.1 was designed to plug into each of the five 10 inch diffuser riser pipes of the 20 mgd ARCADIS design in The Master Plan. Each 10 inch riser pipe receives 4 mgd from a 54 inch diameter feeder pipe buried below the seafloor that delivers the brine discharge to 5 diffuser risers. In the 20 mgd ARACADIS design in the Master Plan, five 4 ft sections of 10 inch riser pipe stand above the seabed and are fitted with a Tideflex duckbill nozzle angled upward at a 60 degree angle, so that each of the Tideflex duckbill nozzles are discharging 4 mgd of brine at 3.4 m/s. In the modified design in Figure 4.1, the 10 inch riser pipes discharges at the seafloor interface into a 9 ft diameter swirl chamber that stands 3.8 ft above the sea floor and is fitted with four rigid 9.5 inch diameter converging nozzles, (each providing roughly the same port cross-sectional area as the Tideflex duckbill nozzles when fully expanded), located in quadrature on the top of swirl chamber. As a result, the 4 mgd of brine that discharges through each riser pipe is divided among four separate discharge nozzles and reduces the maximum axial discharge velocity from each of the four quadrature discharge nozzles to $u_{\max}$ = 0.95 m /s, or about one-forth the maximum discharge velocities of the 20 mgd ARACADIS design in the Master Plan. This satisfies the threshold impact velocity criteria ($u_{\max} \leq 1$ m/ses) of Cada and Glenn (2001) and Cada et al (2006) to eliminate impact mortality.

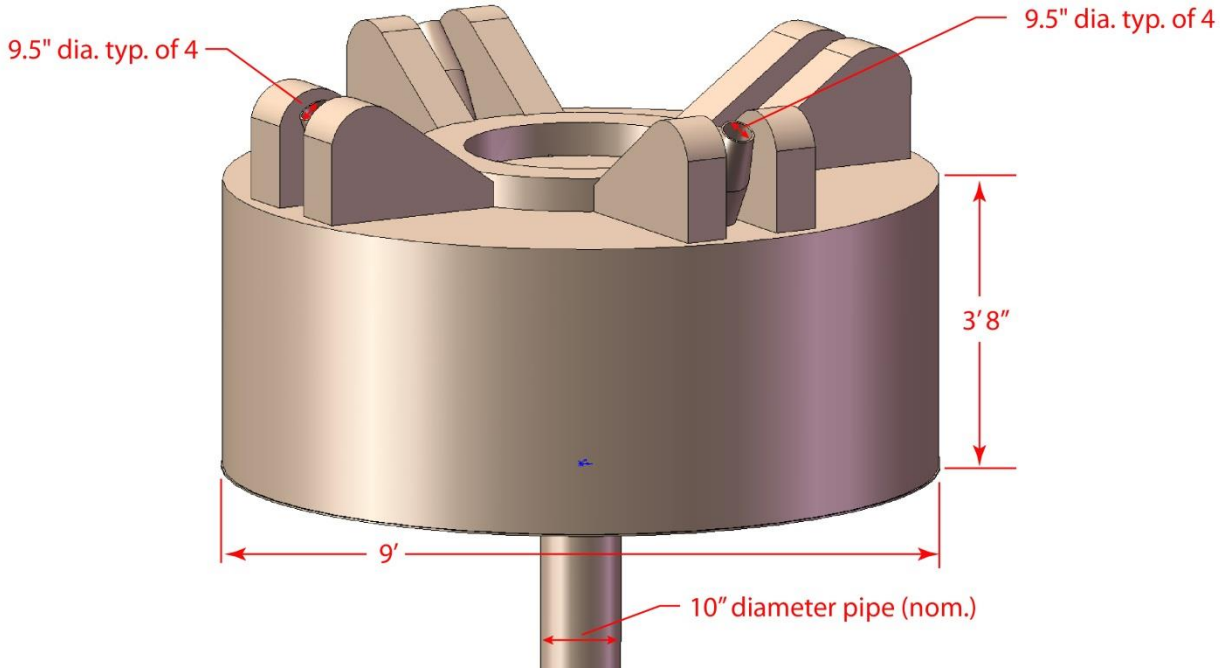

Figure 4.1: Redesigned Phase-1 riser/diffuser to minimize turbulence mortality (typical of 1 of five riser/diffusers). Features 9 ft diameter "swirl chamber" with four 0.9 in. discharge ports angled at 60^0 from horizontal and protected by four pairs of "skid plates" atop the "swirl chamber". The swirl chamber stands 3.8 ft above the ambient seabed and connects at its base with the 10 " riser pipe of the original ARCADIS Phase-1 design. We will refer to this design as the *Four-jet Rosetta Swirl-Chamber Diffuser*.

The 3.8 ft high-stand of the swirl chamber above the seafloor isolates the discharge nozzles from large sand level variations or burial effects. Four pairs of "skid plates" atop the swirl chamber protect the converging nozzles from damage due bottom debris moving about in the wave surge or from boats dragging anchors. However, this configuration still allows divers to reach into the gap between the skid plates to service or replace the nozzles when needed.

Because the modified 20 mgd diffuser concept shown in Figure 4.1 reduces the maximum discharge velocities by a factor of 4 relative to the original ARCADIS design in The Master Plan, the concern becomes whether or not it will produce adequate turbulence in the turbulent mixing zone in order to satisfy the water quality objects of either the Present version of The Ocean Plan, or the 5% Rule under a potential amendment to The Ocean Plan. The purpose of the swirl chamber in Figure 4.1 is to pre-empt turbulence formation in the brine effluent prior to discharge, rather than relying entirely on velocity shear between the discharge jet and the receiving water to generate turbulence, as occurs in the conventional ARCADIS design. The swirl chamber creates high in-the-pipe turbulence levels prior to discharge by two mechanisms. The first mechanism results from the very rapid flow divergence which occurs when the brine is discharged from the10 inch riser pipe into the 9 ft diameter swirl chamber. This produces a rapid deceleration of the brine effluent against a large adverse pressure gradient inside the swirl chamber, a combination which produces flow instability and turbulence formation (Schlichting and Gersten, 1999). The second turbulence generating mechanism at work inside the swirl chamber is produced by a helical internal ribbing on the inner walls of the swirl chamber (see Figure 4.2). This ribbing works like a screw, and causes the mass of brine fluid inside the chamber to rotate as it flows from the bottom of the chamber to eventually exit out the top

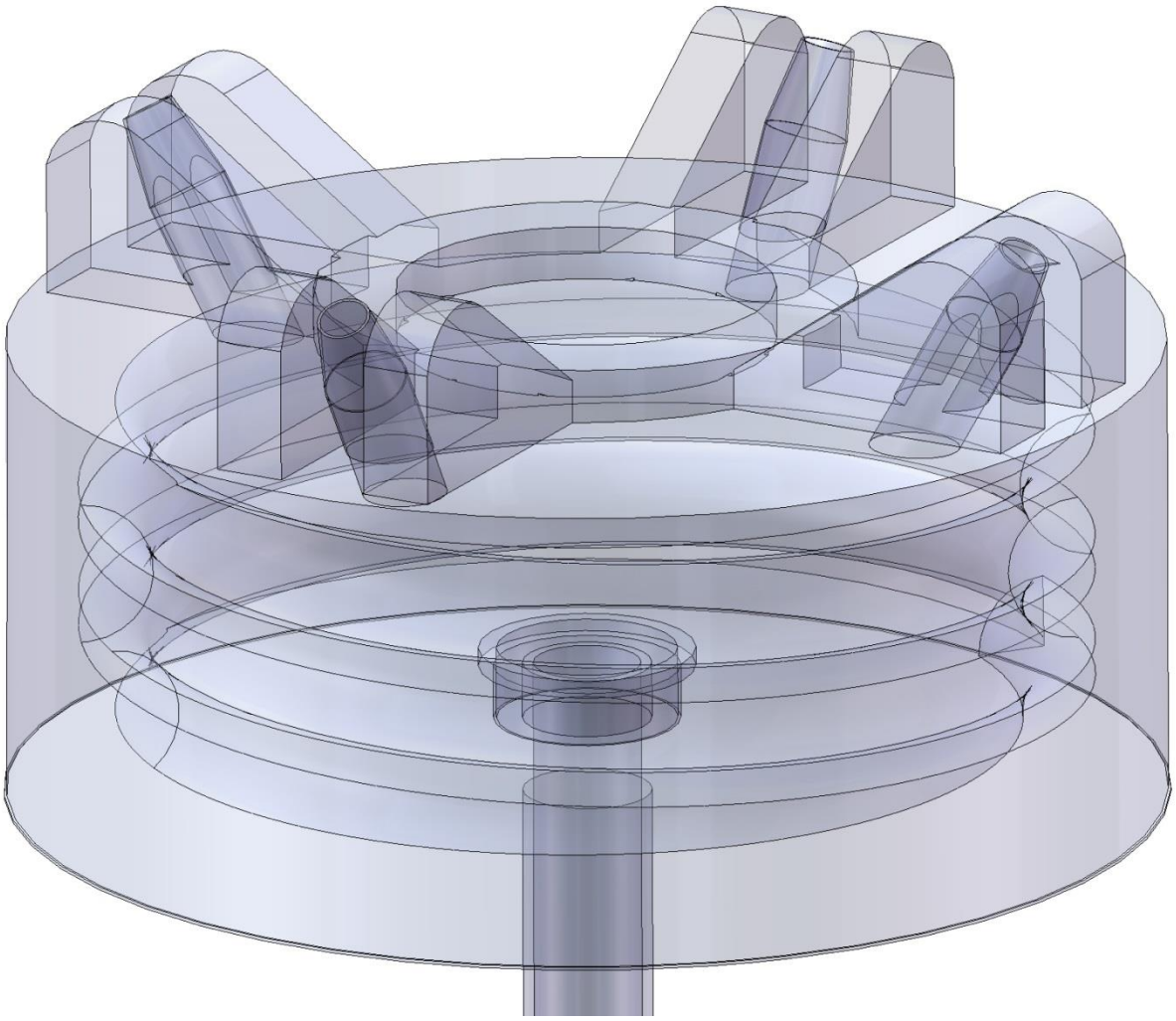

Figure 4.2: Transparent view of the redesigned Phase-1 riser/diffuser (Four-jet Rosetta Swirl-Chamber Diffuser) showing helical internal ribbing on the inner walls of the swirl chamber to provoke turbulent cascading of mixing lengths prior to discharge.

where the four discharge nozzles are located. The combined action of the flow divergence and flow rotation that occurs inside of the swirl chamber produces a turbulent brine effluent and provokes *turbulent cascading* to smaller mixing lengths prior to discharge (Schlichting and Gersten, 1999).

The pre-mature formation of high turbulence levels in the brine effluent inside the swirl chamber consumes flow energy, energy that must be provided by higher operating pressures in the discharge pipeline. To evaluate the higher pressure gradient requirements in the discharge pipeline with the modified 20 mgd diffuser concept shown in Figure 4.1, ARCADIS engineering drawings of the discharge hydraulic infrastructure were gridded into a series of lattice panels to form a nearfield grid as shown in Figure 4.3. Figure 4.3 shows a cross-section simulation of brine discharge from four of the five low-velocity Rosetta diffusers fitted to the the buried 54-inch feeder pipe of the 20 mgd Phase-1 design. The feeder pipe distributes 4 mgd to each 4-jet Rosetta diffusers. Velocities steadily drop along the length of the feeder pipe while the back-pressures rise, increasing the pressure gradient required to drive the system against the ambient ocean pressure. Some additional pressure head-losses are apparent at the junction of the feeder pipe with the riser pipe. The simulation in Figure 4.3 was based on discharge into a perfectly quiet ocean with no waves or current motion in the receiving water. The aggregate results of these “quiet-ocean” simulations indicate that the pressure requirements to drive the discharge hydraulic infrastructure against ambient ocean pressure increase from 6 psi over ambient for the 20 mgd ARACADIS design in The Master Plan to 8 psi over ambient when each of the five risers is fitted with the modified 20 mgd Four-jet Rosetta Swirl-Chamber Diffuser concept.

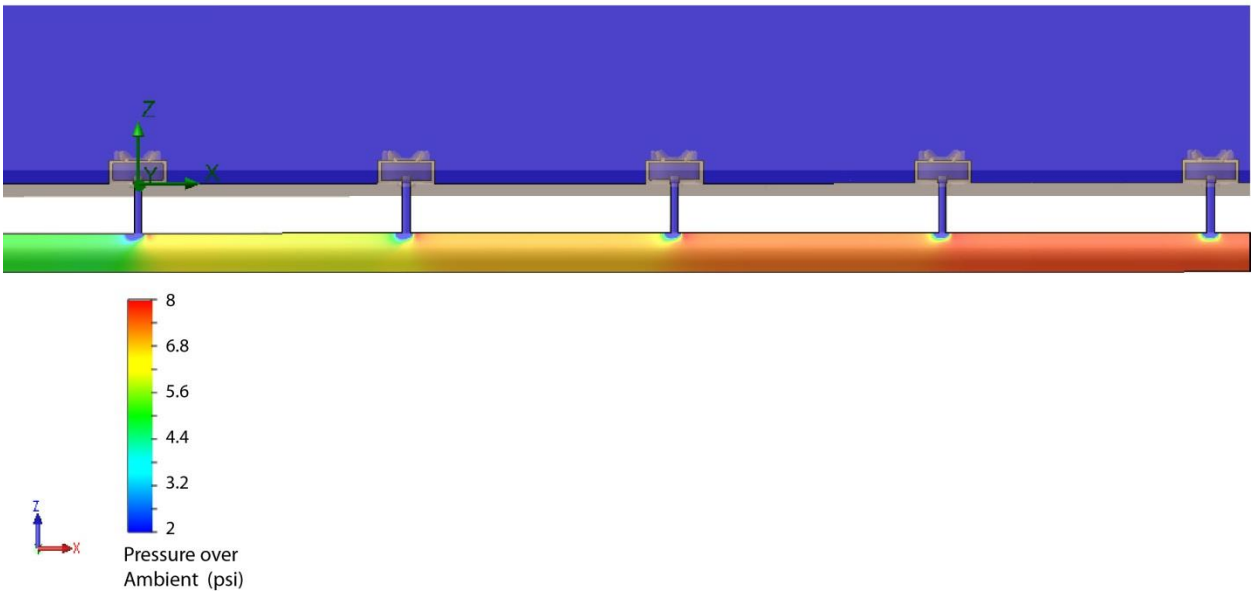

Figure 4.3. "Quiet Ocean" simulation of internal pipe flow through four of five of redesigned Phase-1 riser/diffuser structures, (referred to as Four-jet Rosetta Swirl-Chamber Diffuser); 4 mgd discharge for each individual Four-jet Rosetta Swirl-Chamber Diffuser.

4.2) Turbulence and Shear Stress of the Rosetta Swirl-Chamber Diffuser

The turbulence and shear stress morphology of the diffuser jets, and kinetics of the turbulent mixing zone resulting there from, was evaluated with the Vortex Lattice Model. Figure 4.4 shows a Vortex Lattice Model simulation of 4 mgd brine discharge from one of five Four-jet Rosetta Swirl-Chamber Diffusers for the 20 mgd Phase-1 project. End-of-pipe salinity of the Phase-1 brine effluent is 67 ppt. Inspection of Figure 4.4 reveals similar flow structures to that found in the higher-velocity single jet discharge in Figure 1.1. The combined discharges from the four low-velocity jets of the Rosetta Swirl-Chamber Diffuser generate turbulent outflow regions angled upward at 60 degrees and surrounding the core of each jet; while turbulent shear between these outflow regions and the surrounding water mass give rise to inflowing entrainment regions. The outflow regions promote turbulent mixing of the brine effluent out to large distances away from the diffuser (turbulent mixing zone), while the inflow regions provide a continuous source of dilution water that is entrained into the four brine discharge streams from considerable distances away from the diffuser. Because these outflowing brine streams are heavier than the receiving water (negatively buoyant), the upward trajectories of the outflow regions collapse and fall back toward the seafloor once the momentum flux of the outflow regions is less than the negative buoyancy of the brine streams.

Figure 4.5 gives a 3-dimensional Vortex Lattice solution of the streamline pattern in the aggregate turbulent mixing zone generated by the combined discharges from all five of the Four-jet Rosetta Swirl-Chamber Diffusers as deployed in the 20 mgd Phase-1 project. Each of the twenty jets in this Phase-1 linear diffuser array discharge 1 mgd each of brine effluent at 67 ppt end-of-pipe salinity. It is clear from Figure 4.5 that these 20 jets create very vigorous mixing in

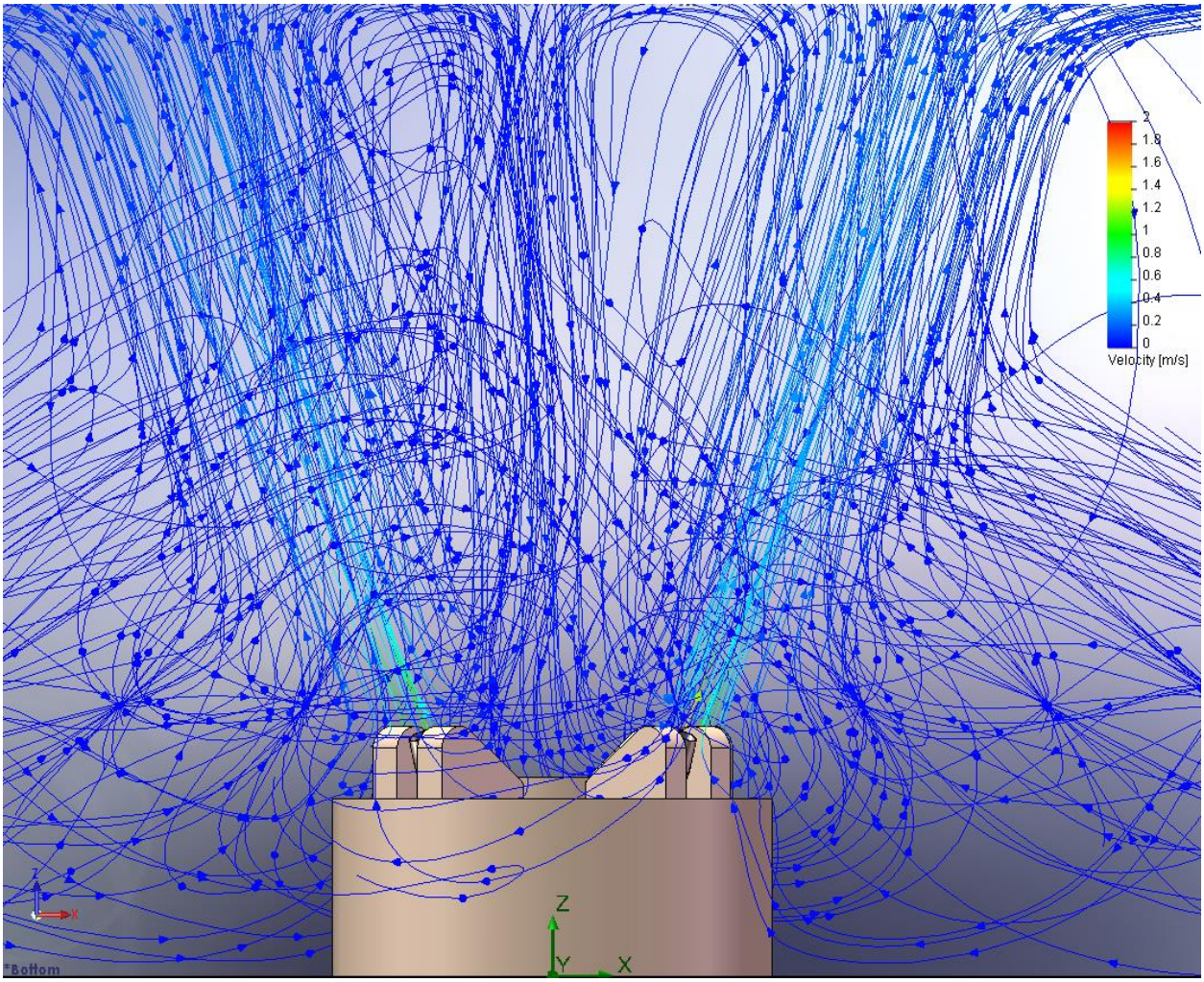

Figure 4.4: Vortex Lattice Model simulation of 4 mgd brine discharge from one of five Four-jet Rosetta Swirl-Chamber Diffusers for the 20 mgd Phase-1 project. Maximum axial velocity from each of the four jets is u_{max} = 0.95 m /s. Maximum shear rates along the outer edges of the high velocity core of each jet are $\frac{d\bar{u}}{dr}$ = 59 sec^{-1} . Brine salinity is 67 ppt.

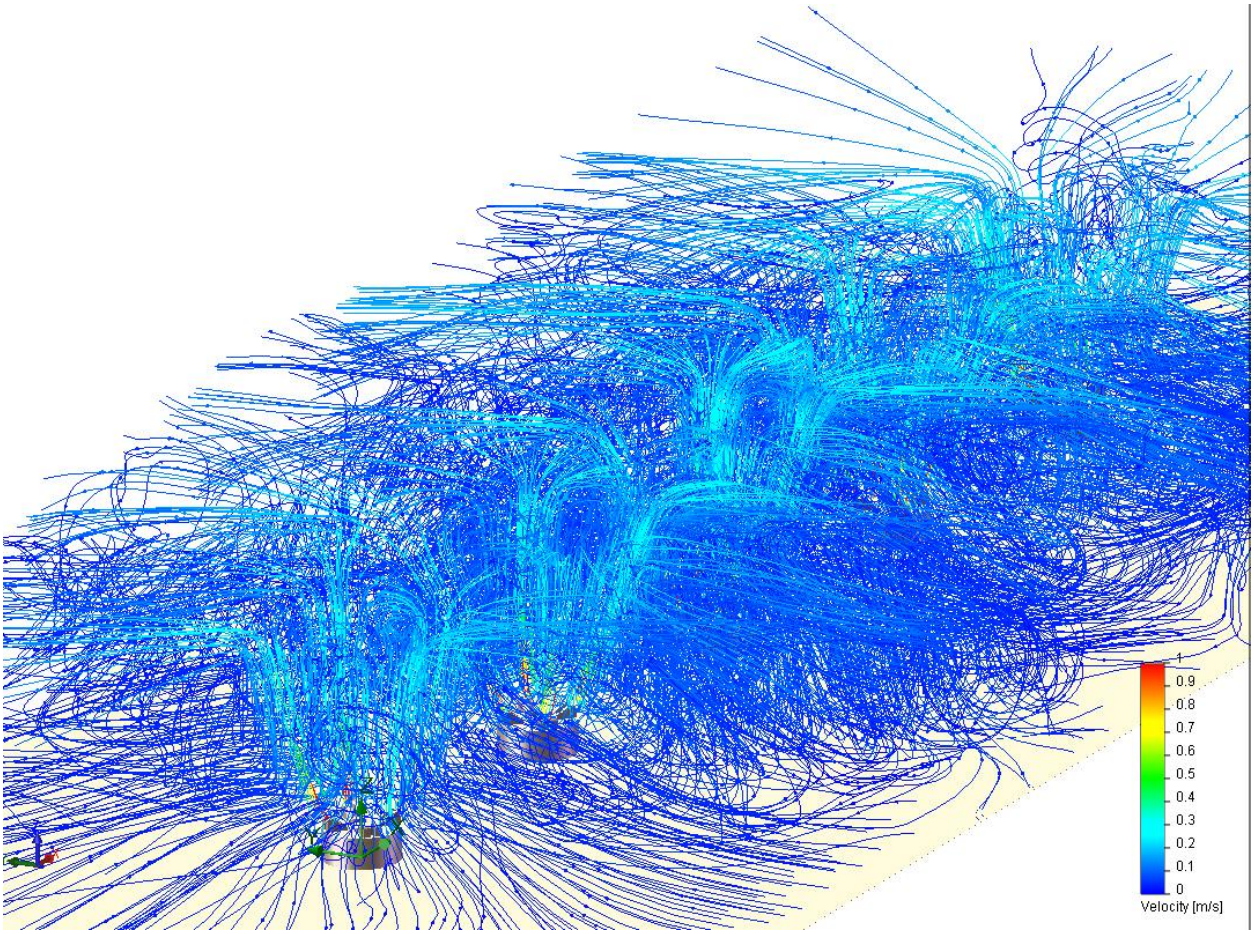

Figure 4.5: Vortex Lattice Model simulation of 20 mgd brine discharge from all five of the Four-jet Rosetta Swirl-Chamber Diffusers for the 20 mgd Phase-1 discharge array using Master Plan spacings and alignments. Maximum axial velocity from each of the 20 jets is $u_{\max}$ = 0.95 m /s. Maximum shear rates along the outer edges of the high velocity core of each jet are $\frac{d\bar{u}}{dr}$ = 59 $\sec^{-1}$. Brine salinity is 67 ppt.

the nearfield of the receiving water, with considerable mutual interaction of the discharge streams of each jet. Furthermore, the quadrature arrangement of the jets on each Rosetta Swirl-Chamber Diffuser produces a turbulent mixing zone having considerable breadth , and consequently ocupies more aggregate volume of the receiving water than would otherwise be possible with a 20 mgd linear array of five single jet diffusers as originally specified for the Phase-1 project in The Master Plan. Maximum velocity anywher in the agregate turbulent mixing zone of Figure 4.5 is $u_{\max}$ = 0.95 m /s; while the maximum shear rate anywhere in the turbulent mixing zone is $\frac{d\bar{u}}{dr}$ = 59 sec^{-1} . Thus the combined discharges from five the Four-jet Rosetta Swirl-Chamber Diffusers at 30 ft. spacings will satisfy the threshold impact velocity criteria ($u_{\max} \leq 1$ m/ses) for eliminating impact mortality, while minimizing turbulent shear mortality by reducing shearing rates to less than $\frac{d\bar{u}}{dr} \leq$ 100 sec $^{-1}$ based on research conducted in the hydroelectic industry for fresh water species after Cada and Glenn (2001) and Cada et al (2006).

The remaining aspect to be consider in reducing turbulent shear mortality is the size of the keystone organisms (mature larvae and juvenile adults) in relation to the turbulence length scales in the aggregate turbulent mixing zone. Figure 4.6 plots the auto spectra of velocity fluctuations, $f(\eta)$ -curve, and cumulative turbulent energy length scale distribution, $F(\eta)$ -curve in the turbulent mixing zone that was computed in Figure 4.5. These spectra and energy distributions are based isotropic turbulence closure relations after Schlichting and Gersten, (1999) applied to the Vortex Lattice CFD solution in Figure 4.5. The autospectra of the turbulent velocity fluctuations peaks at 0.07 mm, identifying the Komogorov turbulent

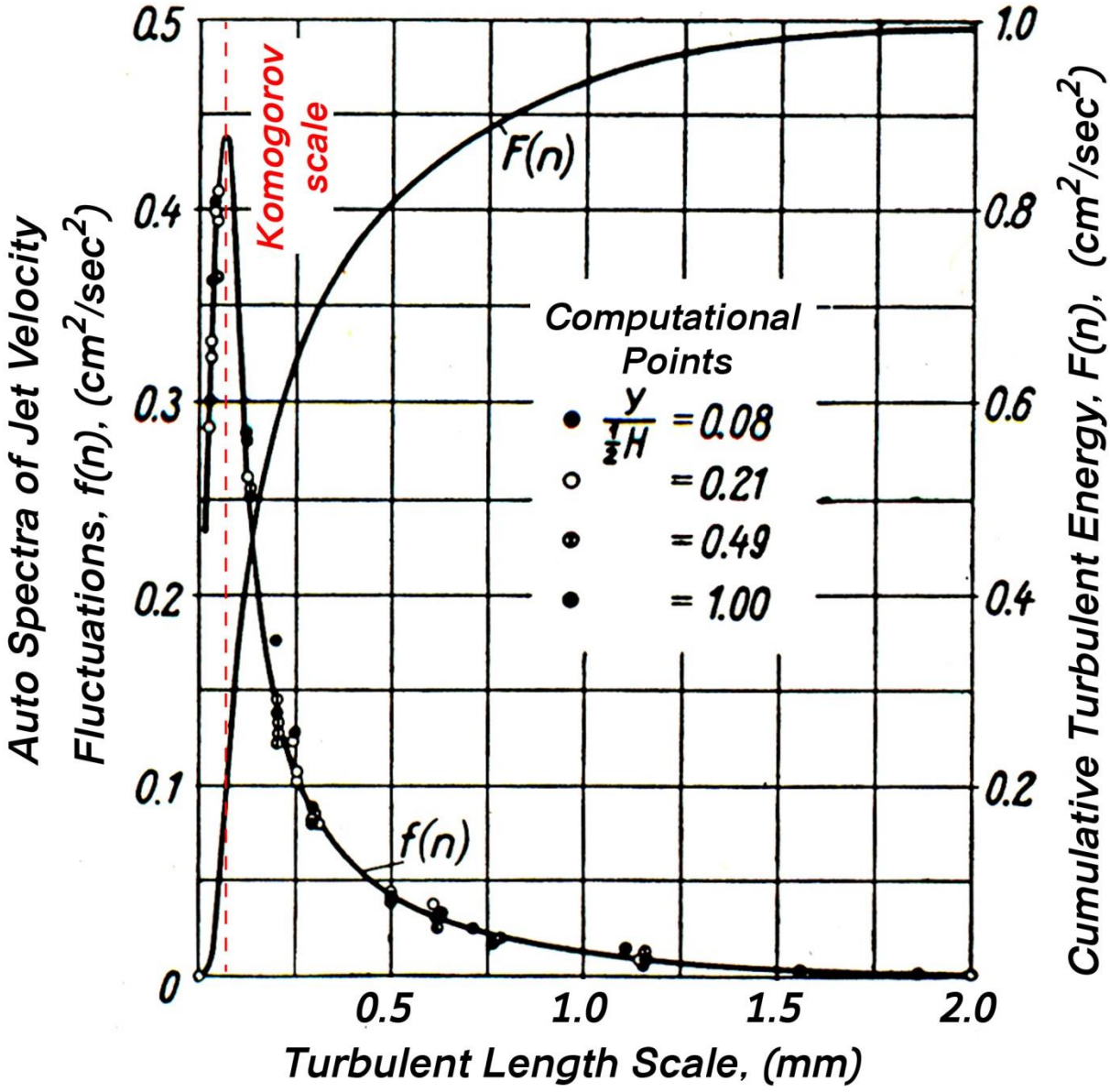

Figure 4.6: Auto spectra of velocity fluctuations and cumulative turbulent energy length scale distribution in the aggregate turbulent mixing zone of five Four-jet Rosetta Swirl-Chamber Diffusers for the 20 mgd Phase-1 project (cf. Figure 4.5). Based on isotropic turbulence closure relations for a free jet after Schlichting and Gersten, 1999. Auto spectra and cumulative turbulent energy normalized by mean flow kinetic energy according to: $f(\eta) = \sum_{i,j} < u_i u_j > / \bar{u}^2$; and $F(\eta) = \sum_{\eta} f(\eta)$

length scale. Consequently the Komogorov length scale is 20 times smaller than the smallest organism (1.5 mm) found in the species size distribution in Figure 3.1. Moreover, the cumulative turbulent energy curve in Figure 4.6 indicates that 99% of the turbulent energy in the turbulent mixing zone of Figure 4.5 occurs at turbulent length scales smaller than the smallest organism (1.5 mm) found in the species size distribution in Figure 3.1. Therefore, the second requirement for minimizing turbulent shear mortality, (ie., that Komogorov turbulent mixing lengths in the diffuser jet are significantly less size of the predominant organisms), has clearly been met by the Four-jet Rosetta Swirl-Chamber Diffuser concept.

4.3) Brine Dilution Performance of the Rosetta Swirl-Chamber Diffuser

Figure 4.7 gives a Visual Plumes one-dimensional simulation of dilution of brine on the seabed for the Phase-1, 20 mgd, using the proposed Four-jet Rosetta Swirl-Chamber Diffuser concept. Visual Plumes has no wave or tidal current transport physics, so the Figure 4.7 result represents Phase-1 dilution in a perfectly quiet ocean with no ambient motion. This is the receiving water condition required for the implementation of the daily maximum acute toxicity receiving water quality objective of 0.3 TUa (acute toxicity units), per Requirement III.C.4(b) of the *California Ocean Plan.* In Figure 4.7 discharge salinity is shown in red and scaled against the right hand axis as a function of radial distance outward from one diffuser jet nozzle, typical of 20 diffuser jets; 4 ea. per discharge riser, (cf Figure 4.1). Dilution factor in Figure 4.7 is plotted in blue according to the left hand axis, also as a function of radial distance outward from one typical of 20 diffuser jets. Under Phase-1, each diffuser jet discharges nominally 1 mgd from the Four-jet Rosetta Swirl-Chamber Diffuser concept. Total Phase-1 discharge is produced by 20 such diffuser nozzles discharging a combined total flow rate of 20 x 1 mgd ea. =

20 mgd total brine discharge at 66.98 ppt (≈ 67.0 ppt) end-of-pipe brine salinity. Ambient ocean salinity is 33.49 ppt (≈ 33.5 ppt) according to Table 3.4 of Jenkins and Wasyl (2012). Figure 4.7 indicates that turbulent mixing and entrainment from a single diffuser nozzle of the Four-jet Rosetta Swirl-Chamber Diffuser concept dilutes brine salinity to 10% over ambient (36.9 ppt) at a distance of only 2.0 m from the point of discharge; and dilutes brine salinity to only 5% over ambient (35.2 ppt) at a distance of only 4.7 m from the point of discharge. A Phase-1 diffuser nozzle dilutes the brine to only 1.2% over ambient ocean salinity at a distance of 15 m from the point of discharge. Although this dilution performance is not as good as the original ARCADIS high velocity diffuser design in the Master Plan; the Four-jet Rosetta Swirl-Chamber Diffuser concept will none the less easily satisfy the discharge requirements of the present version of the California Ocean Plan, as well as the proposed 5 % rule amendment.

Figure 4.8 gives a three-dimensional SEDEXPORT model solution of salinity contours of the mass of *new water* introduced into the nearfield of the receiving water as 20 mgd of brine discharge at 67 ppt end-of-pipe by the combined discharges from 5 ea. of the Four-jet Rosetta Swirl-Chamber Diffusers in the Phase-1 layout. The salinity contour color bar scale is on the left hand side of Figure 4.8, and the cross-shore distance scale is along the backside of the nearfield grid. Comparing Figure 4.8 with Figure 4.7 it is clear that there are minor collective discharge effects among the 20 diffuser jets that retard dilution, particularly in the longshore direction. The combined discharge plumes from the 20 jets tend to spread in the longshore direction under the influence of the tidal drift, which in worst case is only 2.7 cm/sec. As a result, the Rosetta Swirl-Chamber Diffusers Phase-1 diffuser layout produces some minor down-drift *hotspots* that appear as a light blue *halos* in Figure 4.8, where brine salinity remains at 5% over ambient (35.2 ppt) at distances as far as 10m from the diffuser

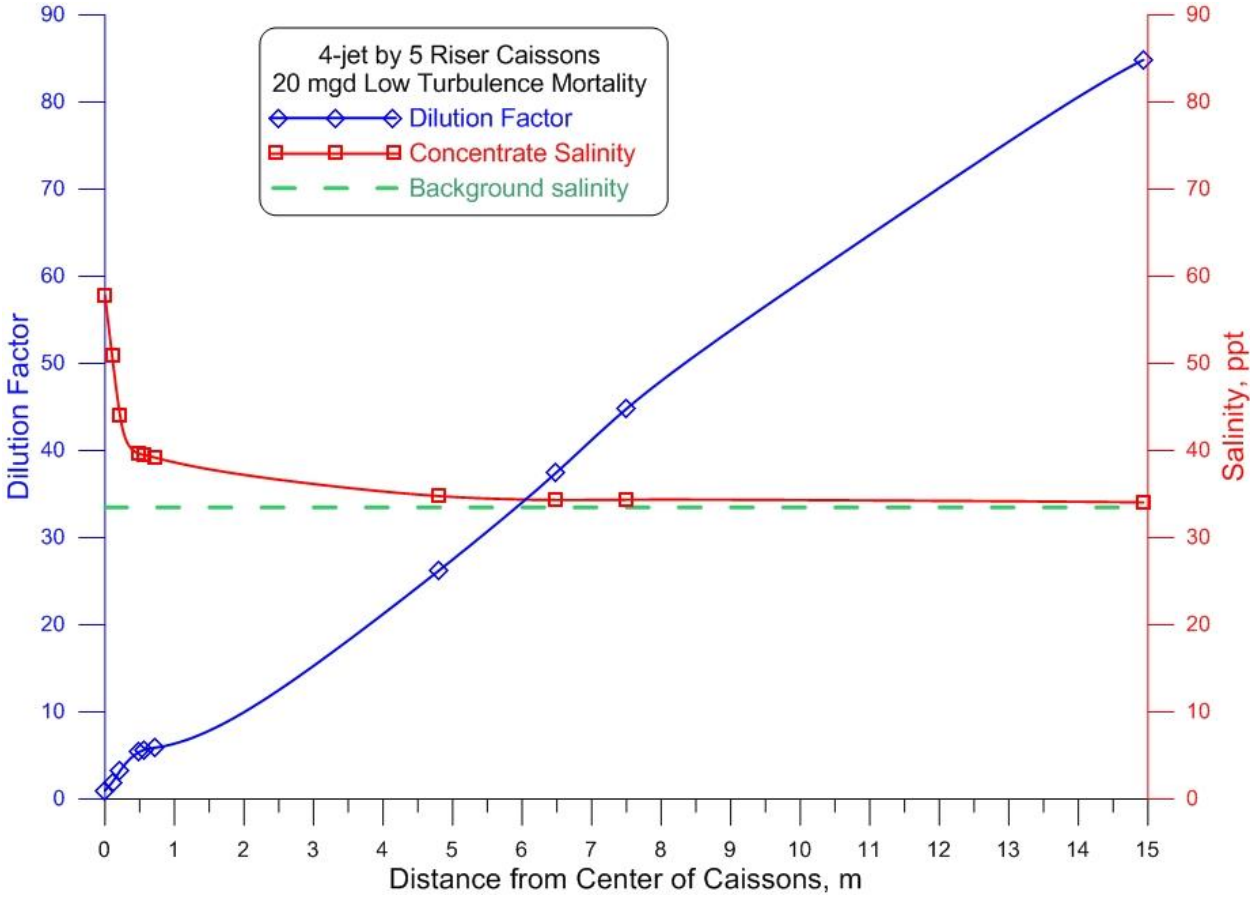

Figure 4.7: Visual Plumes one-dimensional simulation of still water dilution of brine discharged from the Four-jet Rosetta Swirl-Chamber Diffuser concept deployed in the 20 mgd Phase-1 project. Solution based on the Phase-1 worst case scenario (cf. Table 3.4, Jenkins and Wasyl, 2012). Discharge salinity on the seabed (red, right hand axis) as a function of radial distance outward from one typical of 20 diffuser jets; 4 ea. per discharge riser, (cf Figure 4.1). Dilution factor on the seabed (blue, left hand axis) as a function of radial distance outward from one typical diffuser jet. Each diffuser jet discharging ~1 mgd. Total Phase-1 discharge: 20 nozzles x 1 mgd ea. = 20 mgd total brine discharge at 67 ppt end-of-pipe.

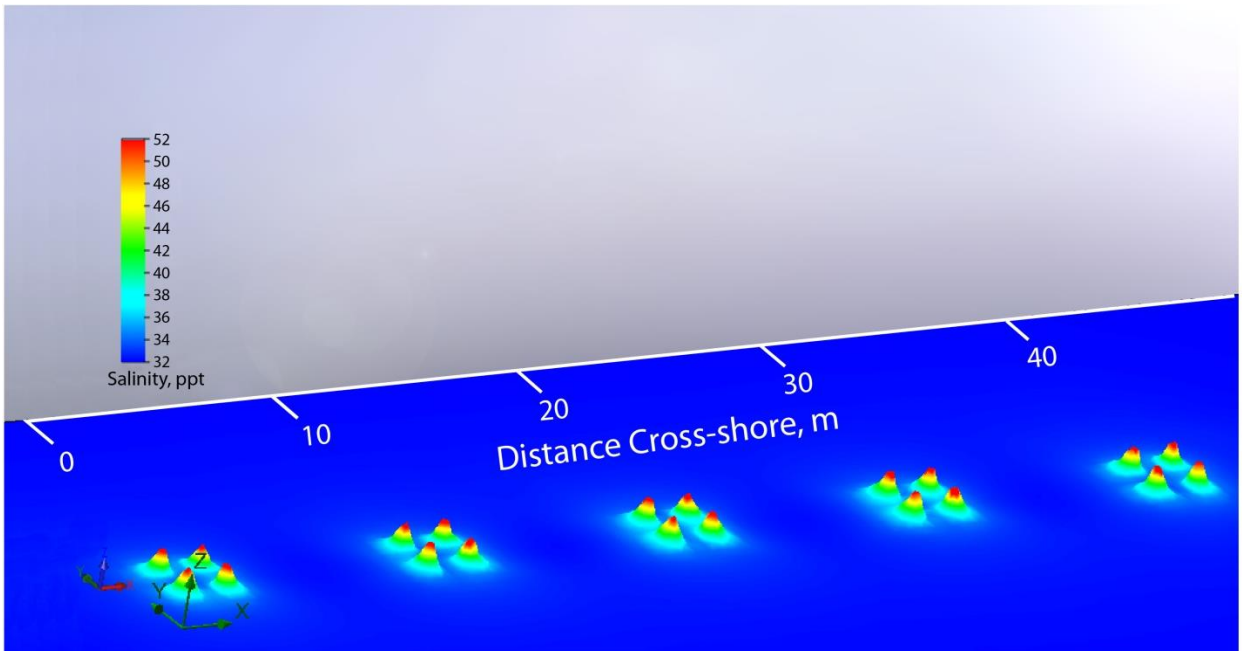

Figure 4.8: SEDXPORT three--dimensional brine plume simulation of dilution/ dispersion from deployment of five ea. of the Four-jet Rosetta Swirl-Chamber Diffusers in the 20 mgd Phase-1 layout. Based on Phase-1 worst case scenario (cf. Table 3.4 of Jenkins and Wasyl, 2012). Total Phase-1 discharge: 4 nozzles x 5 risers x 1 mgd ea. = 20 mgd total brine discharge at 67 ppt end-of-pipe.

complex. However, these 3-dimensional hotspots are a non-factor with respect to compliance with discharge requirements of either the present version of the California Ocean Plan, or the proposed 5 % rule amendment. In addition, none of the Phase-1 discharge plumes in Figure 4.8 broach the sea surface at either of the Redondo or El Segundo sites, which represents an improvement over the original ARCADIS high velocity diffuser design, whose brine plumes broached the surface at the shallow Redondo Beach site (cf. Jenkins and Wasyl, 2012).

Additional physical stress to entrained eggs and larvae in turbulent mixing zone of a diffuser jet can arise from contact with very high salinity, because the diffuser does not produce its full initial dilution until the outer edges of the mixing zone. This is a hypersaline toxicity effect dependent on the dose; that is the salinity level integrated over exposure time. Because of the outflow region of the turbulent mixing zone (Figure 4.5), and augmentation by drift rates from ambient ocean currents, exposure time to elevated salinity for these pelagic organisms is generally brief (Figure 4.9); on the order of minutes and significantly less than the exposure time in traditional wet-lab testing. Inspection of Figure 4.9 reveals that exposure times at the very high salinity levels (45 ppt to 55 ppt) are about 5 minutes longer with the *Four-jet Rosetta Swirl-Chamber Diffuser* (blue), as compared to the ARCADIS Phase-1 diffuser (red). Again this reflects the slightly reduced dilution performance of the *Four-jet Rosetta Swirl-Chamber Diffuser* (blue) relative to the ARCADIS Phase-1 diffuser (red), although the exposure times for both designs are less than 1 hour at 45 ppt and less than 10 minutes at 55 ppt.

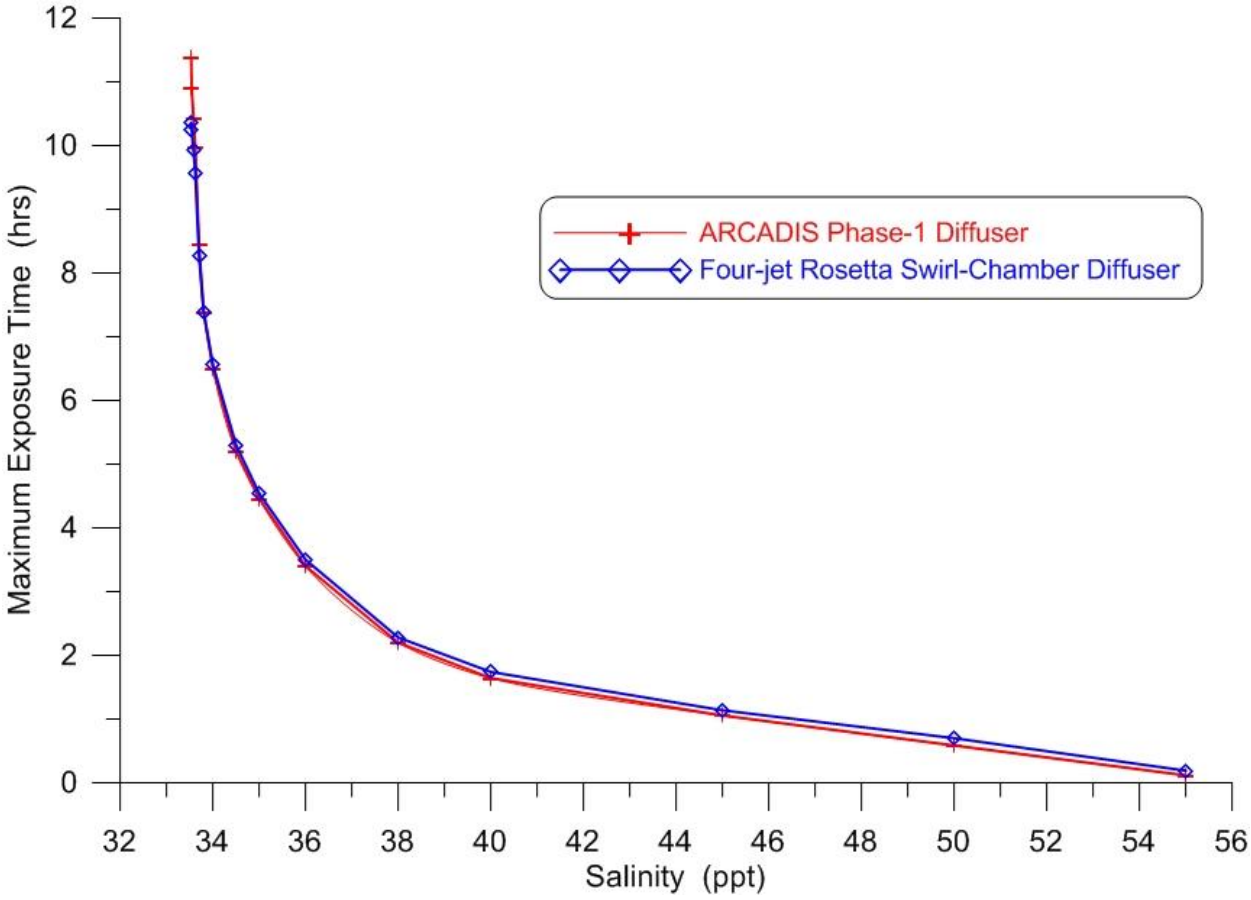

Figure 4.9: Maximum exposure time as a function of salinity for drifting organisms passing through the brine plume of the ARCADIS Phase-1 diffuser (red) as compared to the *Four-jet Rosetta Swirl-Chamber Diffuser* (blue).

5) Conclusions

Published evidence is reviewed herein indicating that physical damage (due to turbulence and velocity shear pulling apart eggs, larva and small juveniles) occurs in open, free-stream turbulent environments, similar to what would occur when these organisms are entrained into the *turbulent mixing zone* of high velocity diffuser systems. We refer to this as *Turbulence Mortality*, and it occurs by two mechanisms. In the turbulent mixing zone of a diffuser, entrained eggs, larvae and

juvenile adults suffer *impact mortality* from direct contact with the high velocity core of a diffuser jet. Along the outer edges of the high velocity core of a diffuser jet, *turbulent shear mortality* occurs along the streamlines between the entrainment and outflow regions of the turbulent mixing zone, where shearing rates in the fluid are very high. Remediation approaches previously applied to hydro-electric turbines, diversion channels and fish ladders by Cada and Glenn (2001) and Cada et al (2006) suggest that impact mortality can be minimized by lowering the velocities in the high speed core of a diffuser jet to a threshold impact velocity of about 1 m/ses; while turbulent shear mortality can be minimized by reducing shearing rates to less than $\frac{d\bar{u}}{dr} \leq 100 \text{ sec}^{-1}$, and by adjusting the Komogorov turbulent mixing lengths in the diffuser jet to significantly less than the size of the predominant organisms. We apply these previously tested remedial criteria to a redesign of the 20 mgd Phase-1diffuser from the Master Plan in order to minimize diffuser induced turbulence mortality.

Our approach to minimizing turbulence mortality is based on a species assessment and size distribution specific to mature larvae and juvenile adults life phases that was measured by Tenera Environmental at the intakes to the Redondo Beach Generating Station (RBGS) and the SeaLife intakes to the West Basin Desalination Demonstration Facility; and from the intakes to the El Segundo Generating Station (ESGS) and Scattergood Generating Station. The size spectra of small organisms in the water column at these sites are very broad. It is not possible to both minimize jet velocity and shearing rate, while simultaneously making the Komogorov turbulent mixing lengths small relative to ***all*** resident water column species and life phases. Therefore it was necessary to prioritize the species size distribution in the Tenera data and focus on mature larvae and juvenile adult life phases. This size class of organism was chosen for this diffuser design

optimization because it accounts for the life phases which have highest survival rates.

Seventeen separate design iterations were conducted with *COSMOS/ FLowWorks* to produce a modified 20 mgd Phase-1 diffuser design that minimizes turbulence mortality to mature larvae and juvenile adults. We refer to this modified design concept as the *Four-jet Rosetta Swirl-Chamber Diffuser* , and it was designed to plug into each of the five 10 inch diffuser riser pipes of the 20 mgd ARCADIS design in The Master Plan. In the modified design, the 10 inch riser pipes discharge at the seafloor interface into a 9 ft diameter swirl chamber that stands 3.8 ft above the sea floor and is fitted with four rigid 9.5 inch diameter low-velocity converging nozzle located in quadrature on the top of swirl chamber. The 3.8 ft high-stand of the swirl chamber above the seafloor isolates the discharge nozzles from large sand level variations or burial effects. Four pairs of "skid plates" atop the swirl chamber protect the converging nozzles from damage due bottom debris moving about in the wave surge or from boats dragging anchors. However, this configuration still allows divers to reach into the gap between the skid plates to service or replace the nozzles when needed.

Because the Four-jet Rosetta Swirl-Chamber Diffuser reduces the maximum discharge velocities by a factor of 4 relative to the original ARCADIS design in The Master Plan, the concern becomes whether or not it will produce adequate turbulence in the turbulent mixing zone in order to satisfy the water quality objects of either the present version of the *California Ocean Plan,* or the *5% Rule* under a potential amendment to The Ocean Plan. The purpose of the swirl chamber is to pre-empt turbulence formation in the brine effluent prior to discharge, rather than relying entirely on velocity shear between the discharge jet and the receiving water to generate turbulence, as occurs in the conventional ARCADIS design. The swirl

chamber creates high in-the-pipe turbulence levels prior to discharge by two mechanisms. The first mechanism results from the very rapid flow divergence which occurs when the brine is discharged from the10 inch riser pipe into the 9 ft. diameter swirl chamber. This produces a rapid deceleration of the brine effluent against a large adverse pressure gradient inside the swirl chamber, a combination which produces flow instability and turbulence formation (Schlichting and Gersten, 1999). The second turbulence generating mechanism at work inside the swirl chamber is produced by a helical internal ribbing on the inner walls of the swirl chamber. This ribbing works like a screw, and causes the mass of brine fluid inside the chamber to rotate as it flows from the bottom of the chamber to the top, where the four discharge nozzles are located. The combined action of the flow divergence and flow rotation that occurs inside of the swirl chamber produces a turbulent brine effluent and provokes *turbulent cascading* to smaller mixing lengths prior to discharge (Schlichting and Gersten, 1999).

The pre-mature formation of high turbulence levels in the brine effluent inside the swirl chamber consumes flow energy, energy that must be provided by higher operating pressures in the discharge pipeline. “Quiet-ocean” CFD pipe flow simulations indicate that the pressure requirements to drive the discharge hydraulic infrastructure against ambient ocean pressure increase from 6 psi over ambient for the 20 mgd ARACADIS design in The Master Plan to 8 psi over ambient when each of the five risers is fitted with the Four-jet Rosetta Swirl-Chamber Diffuser concept.

The quadrature arrangement of the jets on each Rosetta Swirl-Chamber Diffuser produces a turbulent mixing zone having considerable breadth , and consequently ocupies more aggregate volume of the receiving water than would otherwise be possible with a 20 mgd linear array of five single jet diffusers, as

originally specified for the Phase-1 project in The Master Plan. With the Rosetta Swirl-Chamber Diffusers, the maximum velocities anywhere in the agregate turbulent mixing zone is u_{max} = 0.95 m /s; while the maximum shear rates anywhere in the turbulent mixing zone is $\frac{d\bar{u}}{dr}$ = 59 sec^{-1} . Thus the combined discharges from five the Four-jet Rosetta Swirl-Chamber Diffusers at 30 ft. spacings will satisfy the threshold impact velocity criteria ($u_{max} \leq 1$ m/sec) for eliminating impact mortality, while minimizing turbulent shear mortality by reducing shearing rates to less than $\frac{d\bar{u}}{dr} \leq$ 100 sec^{-1} Moreover, Komogorov turbulent length scales in the agregate turbulent mixing zone of five Rosetta Swirl-Chamber Diffusers are 20 times smaller than the smallest organism (1.5 mm) found in the Tenera species size distribution. Additionally, 99% of the turbulent energy in the agregate turbulent mixing zone occurs at turbulent length scales smaller than the smallest organism (1.5 mm). Therefore, all requirements for minimizing impact mortality and turbulent shear mortality have been satisfied by the Four-jet Rosetta Swirl-Chamber Diffuser concept, according to the minimization criteria set forth in Cada and Glenn (2001) and Cada et al (2006) that was based on research conducted in the hydroelectic industry for fresh water species.

None of the brine plumes from the Four-jet Rosetta Swirl-Chamber Diffusers will broach the sea surface at either of the Redondo or El Segundo sites. This represents another improvement over the original ARCADIS high velocity diffuser design, whose brine plumes broached the surface at the shallow Redondo Beach site. Dilution performance of the Four-jet Rosetta Swirl-Chamber Diffuser is not as good as the original ARCADIS high velocity diffuser design in the Master Plan. The Four-jet Rosetta Swirl-Chamber Diffuser concept will none the less

easily satisfy the discharge requirements of the present version of the California Ocean Plan, as well as the proposed 5 % rule amendment. Exposure times of drifting organisms to the brine plumes at very high salinity levels (45 ppt to 55 ppt) are about 5 minutes longer with the *Four-jet Rosetta Swirl-Chamber Diffuser*, as compared to the ARCADIS Phase-1 diffuser, although the exposure times for both designs are less than 1 hour at 45 ppt and less than 10 minutes at 55 ppt.

The Four-jet Rosetta Swirl-Chamber Diffuser was derived from turbulence mortality minimization criteria developed for fresh water species. The decisive question remains whether or not those citeria are valid for relevant local marine species. We recommend that the State Water Resources Control Board examine this question further.

6) References and Bibliography:

Armi, L. A., 1979, "Effects of variations in eddy diffusivity on property distributions in the oceans," *Jour. of Mar. Res.*, v. 37, n. 3, p. 515-530.

Bograd, S. , Chereskin, T., and D. Roemmich, 2001, "Transport of mass, heat, salt and nutrients in the southern California current system", *Journal of Geophysical Research*, vol 106, no C5, pp 9255-9275

Berkoff, J. C. W., 1972, "Computation of combined refraction-diffraction," *Proc. 13th Coastal Eng. Conf.*, p. 471-490.

Boas, M. L., 1966, *Mathematical Methods in the Physical Sciences,* John Wiley & Sons, Inc., New York, 778 pp., 1966.

Cada, Glenn F.,2001, "The Development of Advanced Hydroelectric Turbines to Improve Fish Passage Survival." *Fisheries*, vol. 26, No. 1. January 2001, pages 14-23.

Cada, Glenn F., James M. Loar, Laura A. Garrison, Richard K. Fisher, and Duane A. Neitzel,2006, "Efforts to Reduce Mortality to Hydroelectric Turbine-Passed Fish: Locating and Quantifying Damaging Shear Stresses," *Environmental Management*, Vol. 37, No. 6, June 2006, pages 898-906.

CDIP, 2004, "Coastal Data Information Program" http://cdip.ucsd.edu/

CRWQCB, 2000, Waste discharge requirements for the AES Redondo Beach Generating Station, NPDES No. CA-0000370, Order No. 00-083.

Connor, J. J. and J. D. Wang, 1973, "Finite element modeling of two-dimensional hydrodynamic circulation," MIT Tech Rpt., #MITSG 74-4, p. 1-57.

Dalrymple, R. A., J. T. Kirby and P. A. Hwang, 1984, "Wave diffraction due to areas of energy dissipation," *Jour. Waterway Port, Coast, and Ocean Engineering*, v. 110, p. 67-79.

Dey, W. 2003. Optimal slot width selection for wedgewire screens, In: Proceedings Report. A Symposia on cooling water intake technologies to protect aquatic organisms, May 6-7, 2003, Arlington VA, USEPA. EPA 625-C-05-002, March 2005.

Durst, C. S., 1924, "The relationship between current and wind," *Quart. J. R.Met. Soc.*, v. 50, p. 113 (London).

EPRI, 2003, *Fish Protection at Cooling Water Intakes: Status Report*, EPRI, Palo Alto, CA, 1999. TR-114013.

EPRI. 2003. Laboratory evaluation of wedgewire screens for protecting early life stages of fish at cooling water intakes. Prepared by Alden Research Laboratory, Inc. EPRI Report No. TR-1005339.

Gallagher, R. H., 1981, *Finite Elements in Fluids*, John Wiley & Sons, New York, 290 pp.

Grant, S.B., J.H. Kim, B.H. Jones, S.A. Jenkins, J. Wasyl, and C. Cudaback, 2005, "Surf zone entrainment, along-shore transport, and human health implications of pollution from tidal inlets," *Jour. Geophys. Res.*, v.110, C10025, doi:10.1029/2004JC002401, 20 pp.

Graham, J. B., 2004, "Marine biological considerations related to the reverse osmosis desalination project at the Applied Energy Sources, Huntington Beach Generating Station," Appendix-S in REIR, 2005, 100 pp.

Hammond, R. R., S. A. Jenkins, J. S. Cleveland, J. C. Talcott, A. L. Heath, J. Wasyl, S. G. Goosby, K. F. Schmitt and L. A. Leven, 1995, "Coastal water clarity modeling," *SAIC*, Tech. Rpt. 01-1349-03-4841-000, 491 pp.

Inman, D. L. and S. A. Jenkins, 1996, "A chronology of ground mine studies and scour modeling in the vicinity of La Jolla," *University of California, San Diego,* Scripps Institution of Oceanography, SIO Reference Series 96-13, 26 pp.

_____S. A. Jenkins and M. H. S. Elwany, 1996, "Wave climate cycles and coastal engineering practice," *Coastal Engineering, 1996, Proc. 25th Int. Conf., (Orlando),* ASCE, New York, v. 1, Ch 25, p. 314-27.

_____and S. A. Jenkins, 1997, "Changing wave climate and littoral drift along the California coast," p. 538-49 in O. T. Magoon et al., eds., *California and the World Ocean '97*, ASCE, Reston, VA, 1756 pp.

Jenkins, S. A. and J. Wasyl, 2004, "Hydrodynamic modeling of source water make-up and concentrated seawater dilution for the ocean desalination project at the AES Huntington Beach Generating Station," Appendix-C in REIR, 2005, 298 pp.

Jenkins, S. A. and J. Wasyl, 2005, "Oceanographic considerations for desalination plants in Southern California coastal waters," Scripps Institution of Oceanography Tech. Rpt. No. 54, 109 pp + appendices. http://repositories.cdlib.org/sio/techreport/54/

Jenkins, S. A. and J. Wasyl, 2005b, "Coastal evolution model," Scripps Institution of Oceanography Tech. Rpt. No. 58, 179 pp + appendices. http://repositories.cdlib.org/sio/techreport/58/

Jenkins, S. A., 2007, "Near-shore Hyper-Saline Effects due to Reduced Flow Rate Scenarios during Stand-Alone Operations of the Carlsbad Desalination Project at Encina Generating Station" submitted to Poseidon Resources, 68 pp

Jenkins, S. A., 2007, "Receiving Water Dilution Analysis for the West Basin Municipal Water District Redondo Beach Temporary Ocean Water Desalination Demonstration Facility" submitted to MWH America, 113 pp.

Jenkins, S. A., Inman, D.L., Michael D. Richardson, M.D., Thomas F. Wever, T.F. and J. Wasyl, 2007, "Scour and burial mechanics of objects in the nearshore", *IEEE Jour.Oc.Eng*, vol. 32, no. 1, pp 78-90.

Jenkins, S. A., 2008a, "Dilution Analysis for Source and Receiving Water for the Santa Cruz Seawater Desalination Project", submitted to Archibald Consulting and the City of Santa Cruz Public Works Department, 104 pp.

Jenkins, S. A. and J. Wasyl, 2008, "Receiving Water Dilution Analysis for the West Basin Municipal Water District Redondo Beach Temporary Ocean Water Desalination Demonstration Facility", submitted to MWH Americas, 10 November 2008, 112 pp.

Jenkins, S. A. and J. Wasyl, 2008, "Wedge-Wire Intake Screen Flow Analysis for the West Basin Municipal Water District Redondo Beach Temporary Ocean Water Desalination Demonstration Facility", submitted to MWH Americas, 28 September 2008, 47 pp.

Jenkins, S. A., 2010, "Potential Impacts on Wave and Current Transport Processes Due to Infiltration Rates Induced by the South Orange Coastal Ocean Desalination Project", submitted to Municipal Water District of Orange County, 18 October, 2010, 13 pp.

Jenkins, S. A., J. Paduan, P. Roberts, D. Schlenk, and J. Weis, 2012,"Management of Brine Discharges to Coastal Waters; Recommendations of a Science Advisory Panel", submitted at the request of the California Water Resources Control Board, 56 pp. + App.

Jenkins, S. A. and J. Wasyl, 2012, "Hydrodynamic Analysis of Intake and Dilution Issues for the West Basin Municipal Water District Sea", submitted to West Basin Municipal Water District, 2 December 2012, 182 pp.

Jerlov, N.G., 1976, *Marine Optics*, Elsevier, Amsterdam, 231 pp.

Jessopp, M.J., "The quick and the dead: larval mortality due to turbulent tidal transport", *J. Mar. Biol. Ass*., UK, vol. 87., pp 675-680.

Kirby, J. T., 1986a, "Higher-order approximations in the parabolic equation method for water waves," *Jour. Geophys. Res.*, v. 91, C1, p. 933-952.

_____, 1986b, "Rational approximations in the parabolic equation method for water waves," *Coastal Engineering*, 10, p. 355-378.

_____, 1986c, "Open boundary condition in the parabolic equation method," *Jour. Waterway, Port, Coastal, and Ocean Eng.*, 112(3), p. 460-465.

Komar, P. D. and D. L. Inman, 1970, "Longshore sand transport of beaches," *Jour. Geophys. Res.*, v. 75, n. 30, p. 5914-5927.

Lazara,B. J. and J. C. Lasheras, 1992a, "Particle dispersion in a developing free shear layer, Part 1, Unforced flow," *Jour. Fluid Mech.* 235, p. 143-178.

Lazara, B. J. and J. C. Lasheras, 1992b, "Particle dispersion in a developing free shear layer, Part 2, Forced Flow," *Jour. Fluid Mech.*, 235, p. 179-221.

List, E. J., G. Gartrell and C. D. Winant, 1990, "Diffusion and dispersion in coastal waters," *Jour. Hydraulic Eng.*, v. 116, n. 10, p. 1158-79.

Longuet-Higgins, M. S., 1970, "Longshore currents generated by obliquely incident waves," *Jour. Geophys. Res.*, v. 75, n. 33, p. 6778-6789.

Master Plan, 2012, "West Basin Municipal Water District Ocean Water Desalination Program Master Plan" ARCADIS, 31 pp.

MBC Applied Environmental Services, 2002, "National pollutant discharge elimination system 2002 receiving water monitoring report AES Redondo Beach L.L.C. Generating Station Los Angeles, California," prepared for AES Redondo Beach L.L.C., 62 pp. + appens.

MBC Applied Environmental Services, 2003, "National pollutant discharge elimination system 2003 receiving water monitoring report AES Redondo Beach L.L.C. Generating Station Los Angeles, California," prepared for AES Redondo Beach L.L.C., 63 pp. + appens.

MBC Applied Environmental Services, 2004, "National pollutant discharge elimination system 2004 receiving water monitoring report AES Redondo Beach L.L.C. Generating Station Los Angeles, California," prepared for AES Redondo Beach L.L.C., 62 pp. + appens.

MBC Applied Environmental Services, 2005, "National pollutant discharge elimination system 2005 receiving water monitoring report AES Redondo Beach L.L.C. Generating Station Los Angeles, California," prepared for AES Redondo Beach L.L.C., 70 pp. + appens.

MBC Applied Environmental Services, 2006, "National pollutant discharge elimination system 2006 receiving water monitoring report AES Redondo Beach L.L.C. Generating Station Los Angeles, California," prepared for AES Redondo Beach L.L.C., 73 pp. + appens.

NCDC, 2004, National Climate Data Center Document Library: http://www4.ncdc.noaa.gov/ol/documentlibrary/datasets.html

Nielsen, P., 1979, "Some basic concepts of wave sediment transport," Series Paper No. 20, *Institute of Hydrodyn. and Hydro. Eng., Tech. Univ. of Denmark.*

NOAA, 2005, "Verified Historic Water Level Data," http://ports-infohub.nos.noaa.gov/hq/data_res.html

Oden, J. T. and E. R. A. Oliveira, 1973, *Lectures on Finite Element Methods in Continuum Mechanics,* The University of Alabama Press.

Oelker, G, 2007, "TSS data from West Basin desalination pilot plant," e-mail report to Dawn Guendert, 6/25/07.

Radder, A. C., 1979, "On the parabolic equation method for water-wave propagation," *J. Fluid Mech.*, 95, part 1, p. 159-176.

Roemmich, D. 1989, "Mean transport of mass, heat, salt and nutrients in southern California coastal waters", *Deep-Sea Research*, vol 36, no 9, pp 1359-1378.

Schmidt, W., 1917, "Wirkungen der ungeordneten Bewegungen im Wasser der Meere und Seen," *Ann. D. Hydr. u. Marit. Meteorol.*, vol. 45, p. 367-381.

Schlichting H.T. and K. Gersten, 1999, *Boundary Layer Theory, 8th Edition,* Springer-Verlag Berlin and Heidelberg GmbH & Co. KG, 687 pp.

Schoonmaker, J. S., R. R. Hammond, A. L. Heath and J. S. Cleveland, 1994, "A numerical model for prediction of sub-littoral optical visibility," *SPIE Ocean Optics XII*, 18 pp.

SIO, 2005, "Shore Stations Program", Scripps Institution of Oceanography, University of California, San Diego 9500 Gilman Drive, La Jolla, California 92093-0218, http://shorestation.ucsd.edu/active/index_active.html

Stommel, H., 1949, "Horizontal diffusion due to oceanic turbulence," *Journal of Marine Research*, v. VIII, n. 3, p. 199-225.

Thorade, H., 1914, "Die Geschwindigkeit von Triftstromungen und die Ekman'sche Theorie," *Ann. D Hydr. u. Marit. Meteorol.*, v. 42, p. 379.

Trussell, R. S., R. R. Sharma, and T. Venezia, 2007, “West Basin Municipal Water District Temporary Ocean Water Desalination Demonstration Project Assessment SEALab Water Quality Assessment,” submitted to MWH, 21 May 2007, 49 pp.

Schmidt, W., 1917, “Wirkungen der ungeordneten Bewegungen im Wasser der Meere und Seen,” *Ann. D. Hydr. u. Marit. Meteorol.*, vol. 45, p. 367-381.

Schoonmaker, J. S., R. R. Hammond, A. L. Heath and J. S. Cleveland, 1994, “A numerical model for prediction of sub-littoral optical visibility,” *SPIE Ocean Optics XII*, 18 pp.

Wang, H. P., 1975, "Modeling an ocean pond: a two-dimensional, finite element hydrodynamic model of Ninigret Pond, Charleston, Rhode Island," *Univ. of Rhode Island, Marine Tech. Rpt.*, #40, p. 1-58.

Weiyan, T., 1992, *Shallow Water Hydrodynamics*, Water & Power Press, Hong Kong, 434 pp.

APPENDIX-A: Species Size Distribution from West Basin and Redondo Beach Generating Station (from Tenera Environmental, 2012)

Taxon	Common Name	Min	Max	Average	Count
Hypsoblennius spp.	combtooth blennies	1.68	13.07	2.28	725
CIQ goby complex	gobies	1.67	15.28	2.63	600
Genyonemus lineatus	white croaker	1.31	9.47	2.67	347
Atherinopsidae (all)	silversides	4.54	10.76	9.27	262
Hypsypops rubicundus	garibaldi	2.07	3.21	2.59	262
Labrisomidae	labrisomid blennies	2.73	7.62	3.94	165
Cottids (all)	smoothhead sculpin	1.92	3.97	2.83	146
Engraulidae (all)	anchovies	1.34	21.76	4.71	144
Gibbonsia spp.	kelpfishes	3.51	17.08	5.49	136
Typhlogobius californiensis	blind goby	2.23	3.25	2.71	126
Pleuronichthys spp. (all)	turbots	1.18	11.09	2.57	108
Gobiesox spp.	clingfishes	2.33	5.21	3.33	87
Seriphus politus	queenfish	1.57	5.67	2.98	85
Paralichthys californicus	California halibut	1.54	7.79	2.78	67
Sciaenidae	croakers	0.96	6.15	1.99	63
Citharichthys spp. (all)	sanddabs	1.60	2.78	2.24	38
Paralabrax spp. (all)	sea basses	1.05	2.82	1.63	29
Parophrys vetulus	English sole	1.93	5.10	2.94	29
Scorpaenidae	scorpion fishes	1.46	6.09	3.34	28
Syngnathidae (all)	pipefishes	6.51	14.42	8.44	28
Clupeidae	herrings	1.21	4.09	2.41	19
Scorpaenichthys marmoratus	cabezon	3.61	4.77	4.27	18
Merluccius productus	Pacific hake	1.99	3.06	2.68	15
Ophidiidae (all)	cusk-eels	1.41	3.07	2.36	15
Sphyraena argentea	Pacific barracuda	1.60	3.05	2.25	15
Pleuronectidae	righteye flounders	1.59	3.94	2.35	14
Oxyjulis californica	senorita	1.00	2.45	1.79	13
Stenobrachius leucopsarus	northern lampfish	2.62	4.01	3.20	13
Oxylebius pictus	painted greenling	3.10	3.63	3.42	12
Rhinogobiops nicholsi	blackeye goby	1.72	2.89	2.33	12
Cheilotrema saturnum	black croaker	1.30	2.98	1.91	10
Menticirrhus undulatus	California corbina	1.51	3.08	1.93	10
Cottidae	sculpins	2.34	3.31	2.68	9
Neoclinus spp.	fringeheads	4.37	5.32	4.69	8
Labridae	wrasses	1.37	2.28	1.78	7
Xystreurys liolepis	fantail sole	1.57	2.63	2.10	7
Zaniolepis spp.	combfishes	2.82	3.81	3.79	7
Halichoeres semicinctus	rock wrasse	1.74	2.05	1.88	5
Rimicola spp.	kelp clingfishes	3.10	6.19	3.89	5
Leptocottus armatus	Pacific staghorn sculpin	4.14	6.25	4.81	4
Bathymasteridae	ronquils	3.17	3.96	3.62	3
Heterostichus rostratus	giant kelpfish	4.98	6.89	5.91	3
Lepidogobius lepidus	bay goby	3.20	5.28	4.00	3
Leuroglossus stilbius	California smoothtongue	4.36	4.75	4.62	3
Medialuna californiensis	halfmoon	2.05	2.34	2.19	3
Pleuronectiformes	flatfishes	1.66	2.36	1.91	3

Semicossyphus pulcher	California sheephead	1.92	2.22	2.10	3
Symphurus atricaudus	California tonguefish	1.59	2.05	1.85	3
Hippoglossina stomata	bigmouth sole	2.86	3.12	2.99	2
Paralichthyidae	sand flounders	2.16	2.97	2.56	2
Peprilus simillimus	Pacific butterfish	1.59	1.65	1.62	2
Sardinops sagax	Pacific sardine	3.61	11.71	7.66	2
Blennioidei	blennies	4.46	4.46	4.46	1
Chaenopsidae	tube blennies	5.94	5.94	5.94	1
Chilara taylori	spotted cusk-eel	2.71	2.71	2.71	1
Chromis punctipinnis	blacksmith	2.31	2.31	2.31	1
Clupeiformes	herrings and anchovies	1.47	1.47	1.47	1
Gillichthys mirabilis	longjaw mudsucker	2.39	2.39	2.39	1
Girella nigricans	opaleye	1.66	1.66	1.66	1
Pleuronectoidei	flatfishes	0.78	0.78	0.78	1
Roncador stearnsii	spotfin croaker	2.64	2.64	2.64	1
Trachurus symmetricus	jack mackerel	2.35	2.35	2.35	1

APPENDIX-B: Species Size Distribution from El Segundo and Scattergood Generating Stations (from Tenera Environmental, 2012)

Taxon	Common Name	Min	Max	Average	Count
Engraulidae (all)	anchovies	1.53	25.14	5.81	318
Sciaenidae	croakers	0.79	6.74	1.56	303
Genyonemus lineatus	white croaker	1.30	14.00	3.39	301
CIQ goby complex	gobies	1.79	12.26	3.69	296
Pleuronichthys spp. (all)	turbots	1.37	6.60	2.43	275
Paralichthys californicus	California halibut	1.21	5.74	1.88	211
Paralabrax spp. (all)	sea basses	0.91	2.67	1.67	198
Stenobrachius leucopsarus	northern lampfish	2.23	4.17	3.16	156
Citharichthys spp. (all)	sanddabs	0.85	24.10	1.72	154
Hypsoblennius spp. (all)	combtooth blennies	1.75	4.92	2.50	144
Seriphus politus	queenfish	1.31	6.14	1.90	137
Sphyraena spp. (all)	barracudas	1.55	3.04	2.31	124
Atherinopsidae (all)	silversides	5.76	12.76	8.07	123
Ophidiidae (all)	cusk-eels	1.52	3.55	2.53	102
Oxyjulis californica	senorita	1.02	2.49	1.78	85
Haemulidae	grunts	1.40	2.53	1.83	81
Parophrys vetulus	English sole	2.13	13.80	3.15	71
Menticirrhus undulatus	California corbina	1.35	3.48	1.82	70
Lepidogobius lepidus	bay goby	2.26	7.12	4.04	50
Cheilotrema saturnum	black croaker	1.35	3.76	2.02	48
Pleuronectidae	righteye flounders	1.14	2.78	1.96	42
Symphurus atricaudus	California tonguefish	1.30	23.43	2.34	38
Xenistius californiensis	salema	1.48	2.35	1.87	35
Anisotremus davidsonii	sargo	1.50	3.28	1.97	29
Halichoeres semicinctus	rock wrasse	1.55	2.25	1.86	29
Xystreurys liolepis	fantail sole	1.45	2.35	1.88	29
Semicossyphus pulcher	California sheephead	1.49	3.07	2.19	26
Merluccius productus	Pacific hake	2.32	3.37	2.90	17
Cottidae (all)	sculpins	2.18	5.61	3.00	13
Hippoglossina stomata	bigmouth sole	2.09	3.48	2.95	13
Paralichthyidae	sand flounders	1.48	2.35	1.98	9
Hypsypops rubicundus	garibaldi	2.30	2.63	2.49	8
Gibbonsia spp.	kelpfishes	3.43	6.69	5.38	7
Leptocottus armatus	Pacific staghorn sculpin	3.90	6.00	5.22	7
Sardinops sagax	Pacific sardine	2.28	4.90	3.79	7
Zaniolepis spp.	combfishes	2.99	3.73	3.43	6
Pleuronectiformes	flatfishes	1.08	2.54	1.87	5
Scorpeanidae	rockfish + thornyheads	2.11	3.97	2.94	5
Chilara taylori	spotted cusk-eel	2.58	3.40	3.04	4
Gillichthys mirabilis	longjaw mudsucker	2.47	3.71	3.11	4
Labridae	wrasses	1.58	1.99	1.76	4
Syngnathus spp.	pipefishes	9.15	12.46	10.45	4
Triphoturus mexicanus	Mexican lampfish	2.16	3.26	2.64	4
Kyphosidae	sea chubs	2.38	2.54	2.44	3
Labrisomidae	labrisomid blennies	3.71	5.73	4.60	3
Microstomus pacificus	Dover sole	4.17	5.06	4.68	3
Typhlogobius californiensis	blind goby	2.57	2.90	2.77	3
Acanthogobius flavimanus	yellowfin goby	4.26	4.31	4.28	2

Gobiesox spp.	clingfishes	3.83	4.16	3.99	2
Myctophidae	lanternfishes	2.42	2.83	2.63	2
Oxylebius pictus	painted greenling	2.58	3.28	2.93	2
Pomacentridae	damselfishes	1.87	2.40	2.13	2
Roncador stearnsii	spotfin croaker	1.72	2.09	1.91	2
Ruscarius creaseri	roughcheek sculpin	5.18	5.96	5.57	2
Atractoscion nobilis	white seabass	2.48	2.48	2.48	1
Bathymasteridae	ronquils	3.98	3.98	3.98	1
Chaenopsidae	tube blennies	5.40	5.40	5.40	1
Chromis punctipinnis	blacksmith	2.50	2.50	2.50	1
Clupea pallasii	Pacific herring	2.45	2.45	2.45	1
Clupeiformes	herrings and anchovies	2.99	2.99	2.99	1
Diaphus theta	California headlight fish	2.61	2.61	2.61	1
Etrumeus teres	round herring	3.74	3.74	3.74	1
Girella nigricans	opaleye	2.01	2.01	2.01	1
Hexagrammidae	greenlings	3.66	3.66	3.66	1
Isopsetta isolepis	butter sole	2.52	2.52	2.52	1
Peprilus simillimus	Pacific butterfish	2.42	2.42	2.42	1
Psettichthys melanostictus	sand sole	2.62	2.62	2.62	1
Rhinogobiops nicholsi	blackeye goby	3.62	3.62	3.62	1